ERDC/CRREL TR-04-25

Cold Regions Research
and Engineering Laboratory

US Army Corps
of Engineers®
Engineer Research and
Development Center

FASST Vegetation Models

Susan Frankenstein and George Koenig

December 2004

ERDC/CRREL TR-04-25
December 2004

FASST Vegetation Models

Susan Frankenstein and George Koenig

Cold Regions Research and Engineering Laboratory
U.S. Army Engineer Research and Development Center
72 Lyme Road
Hanover, New Hampshire 03755

Prepared for U.S. Army Corps of Engineers
Washington, DC 20314-1000

ABSTRACT

The one-dimensional dynamic state of the ground model FASST (Fast All-season Soil Strength) is a state of the ground model developed by Frankenstein and Koenig (2004) as part of the Army's Battlespace Terrain Reasoning and Awareness (BTRA) research program. In its original form, the only effects vegetation had on FASST were to change the surface albedo and emissivity. Recently, a two tier, multilayer vegetation algorithm was added. These can be implemented separately or together. Both alter the soil surface energy and moisture budgets. In this report we will discuss the energy balance equations used to solve for the low vegetation, canopy and ground temperatures. In solving these equations, the effects of precipitation interception and soil moisture modification attributable to root-uptake are incorporated.

CONTENTS

ILLUSTRATIONS

TABLES

PREFACE

This report was prepared by Dr. Susan Frankenstein, Research Physical Scientist, Geophysical Sciences Branch, and George Koenig, Research Physical Scientist, Geophysical Sciences Branch, U.S. Army Engineer Research and Development Center, Cold Regions Research and Engineering Laboratory.

Technical review was provided by J. Ballard, U.S. Army Engineer Research and Development Center, Environmental Laboratory, and J. Hardy, Geophysical Sciences Branch, Cold Regions Research and Engineering Laboratory. Funding was provided by Headquarters, U.S. Army Corps of Engineers under the AT42 research program.

This report was prepared under the general supervision of Dr. Richard Detsch, Chief, Geophysical Sciences Branch, and Dr. Lance Hansen, Deputy Director, and James Wuebben, Acting Director, CRREL.

The Commander and Executive Director of the Engineer Research and Development Center is COL James R. Rowen, EN. The Director is Dr. James R. Houston.

LIST OF VARIABLES

Chapter 1

f subscript indicating low foliage (vegetation) terms

g subscript indicating ground terms

α_f , α_g shortwave albedo (0–1)

δ_c calculation variable for E_p

Δt time step (s)

Δz thickness of the surface node (m)

ε_f , ε_g longwave emissivity (0–1)

ε_l calculation variable

γ_p precipitation density (kg/m^3)

Γ_h sensible heat exchange stability correction factor

Γ_e latent heat exchange stability correction factor

κ surface soil thermal conductivity (W/m·K)

ν amount of water flowing towards/away from the surface (m/s)

θ_k change in volumetric ice content at the surface

θ_{max} maximum soil moisture content (m^3/m^3)

θ_p soil moisture content at node p (m^3/m^3)

θ_r residual soil moisture contents (m^3/m^3)

$\overline{\theta}$ average root soil water content (m^3/m^3)

ρ_a air density at the instrument height (kg/m^3)

ρ_{af} density of air near the atmosphere/foliage interface (kg/m^3)

ρ_{ag} density of air near the foliage/ground interface (kg/m^3)

ρ_f air density in the foliage (kg/m^3)

ρ_i ice density (916.5 kg/m^3)

ρ_w water density (1000.0 kg/m^3)

σ Stefan-Boltzman constant (5.699×10^8 W/m^2·K^4)

σ_f fractional coverage (0 – 1)

$\sigma_{f,min}$ minimum fractional coverage (0 – 1)

$\sigma_{f,max}$ maximum fractional coverage (0 – 1)

a calculation variable for vapor pressure

a_f^{ir} longwave absorptivity (0 – 1)

a_r calculation variable for root fraction (m^{-1})

b calculation variable for vapor pressure (K)

b_r calculation variable for root fraction (m^{-1})

c_p specific heat of precipitation (J/kg·K)

$c_{p,w}$ specific heat of water (4217.7 J/kg·K)

$c_{p,i}$ specific heat of ice ($-13.3 + 7.80T_a$ J/kg·K)

$c_{p,a}$ specific heat of air (1005.6 J/kg·K)

C_e^g bulk transfer coefficient for latent heat near the ground

C_{en}^g bulk transfer coefficient near the ground for near neutral conditions

C_f bulk transfer coefficient for turbulent heat in the foliage

C_{hn}^f bulk transfer coefficient at the top of the foliage for near neutral conditions

C_h^g bulk transfer coefficient for sensible heat near the ground

C_{hn}^g bulk transfer coefficient near the ground for near neutral conditions

c_1^f, c_2^f, c_3^f calculation variables

c_1^g, c_2^g, c_3^g calculation variables

d_{max} maximum dew depth on the foliage (mm)

d_1 calculation variable

D precipitation that drips from the foliage (m)

e_a air vapor pressures (Pa)

e_a^0 saturation vapor pressure at 0°C ($e_a^0 = 610.78$ Pa)

$e_{f,sat}$ saturated foliage vapor pressures (Pa)

e_0 windless sensible heat correction factor (2.0 W/m^2)

E_f evaporatation rate (m)

E_p potential evaporation (m/s)

E_{tr} transpiration rate (m)

$E_{tr,max}$ maximum transpiration rate (m)

ff calculation variable for $E_{tr,max}$

f_1, f_2, f_3 calculation variables

F_f sum of energy terms at the atmosphere/foliage interface

g gravitational constant (9.81 m/s^2)

g_D calculation variable for stomatal resistance (10^{-2} Pa^{-1})

H_f sensible heat at the atmosphere/foliage interface (W/m^2)

H_g sensible heat at the foliage/ground interface (W/m^2)

I intercepted precipitation (m)

$I_{ir}^{\downarrow}$ total incoming infrared radiation (W/m^2)

$I_s^{\downarrow}$ total incoming solar radiation (W/m^2)

l latent heat (J/kg)

l_{evap} latent heat of evaporation (J/kg)

l_{sub} latent heat of sublimation (2.838×10^6 J/kg)

l_{fus} latent heat of fusion (2.838×10^6 J/kg)

L_f latent heat at the atmosphere/foliage interface (W/m^2)

L_g latent heat at the foliage/ground interface (W/m^2)

LAI foliage Leaf Area Index (m^2/m^2)

LAI_{min} minimum foliage Leaf Area Index (m^2/m^2)

LAI_{max} maximum foliage Leaf Area Index (m^2/m^2)

$m-1$ subscript indicating previous time step

M_g ground moisture factor ($0 \le M_g \le 1$)

P precipitation heat flux (W/m^2)

P_a atmospheric pressure measured at Z_a (Pa)

P_f precipitation heat at the atmosphere/foliage interface (W/m^2)

P_g precipitation heat at the foliage/ground interface (W/m^2)

P_r precipitation rate (m/s)

$P_{r,g}$ precipitation rate at the ground (m/s)

q_a mixing ratio of air above the foliage

q_{af} mixing ratio of the air at the foliage interface

q_f mixing ratio of air at the top of the foliage

q_g mixing ratio of air at the ground surface

$q_{g,sat}$ saturated ground mixing ratio

$q_{f,sat}$ saturated foliage mixing ratio

r_a atmospheric resistance to water vapor diffusion (s/m)

r_{ce} turbulent Prandtl number (0.71)

r_{ch} turbulent Schmidt (0.63)

r_s stomatal resistance to vapor diffusion (s/m)

$r_{s,min}$ minimum stomatal resistance to vapor diffusion (s/m)

r'' foliage surface wetness factor

R gas constant for air

R_f, R_g surface reflectance ($1 - \varepsilon_f$, ε_g)

R_{ib} bulk Richardson number

R_p fraction of roots at soil node p

RH relative humidity (%)

S_c precipitation stored on the foliage (m)

$S_{c,max}$ maximum stored precipitation on the foliage (m)

SAI Stem Area Index (m^2/m^2)

T_a air temperature at the shelter height Z_a (K)

T_{af} air temperature in the foliage (K)

T_f, T_g temperature (K)

T_p precipitation temperature (K)

T_2 soil temperature just below the surface (K)

u_* friction velocity (m/s)

$\overline{u(z)}$ mean wind speed (m/s)

U_p mass precipitation flux ($kg/m^2 \cdot s$)

W wind speed at the instrument height Z_a (m/s)

W_{af} wind speed at the air–foliage interface (m/s)

W' adjusted wind speed (W' = 2.0 m/s if W is below 2.0 m/s)

z_p depth of node p (m)

z_0^c canopy roughness length (m)

z_0^f foliage roughness length (m)

z_o^g ground roughness length (m)

Z_a shelter/instrument height for air temperature (m)

Z_d zero displacement height (m)

Z_f height (m)

Z_{rh} shelter/instrument height for relative humidity (m)

Z_u shelter/instrument height for wind speed (m)

Chapter 2

c subscript indicating canopy (tree) terms

i superscript/subscript indicating radiation source (1 = sky, 2–4 = canopy, 5 = ground)

j superscript/subscript indicating radiation sink (1 = sky, 2–4 = canopy, 5 = ground)

α_g shortwave albedo of the ground (0–1)

ε_g ground emissivity (0–1)

ε_c^i canopy emissivity of layer i (0–1)

ϕ_k' calculation variable used to calculate leaf slope distributions

γ_p precipitation density (kg/m^3)

θ_k leaf slope angle

θ_r, ϕ_r source angles

ρ_{ac}^i air density at the air–canopy interface (kg/m^3)

σ Stefan-Boltzman constant (5.699×10^{-8} W/m^2·K^4)

σ_c^i canopy density (area/area)

Ψ^i calculation variable related to shortwave albedo (0–1)

$\hat{a}$ unit vector representing the orientation of a leaf at leaf slope angle θ_k

a_c^i canopy shortwave absorption of layer *i* (0 – 1)

A_c^i longwave absorption coefficients of layer *i* (0 – 1)

B_i radiosity of layer *i*

c_p specific heat of precipitation (J/kg·K)

$c_{p,a}$ specific heat of air (1005.6 J/kg·K)

C_c^i bulk transfer coefficient for turbulent heat in the canopy

C_{ijk} the fraction of emitted flux from a source layer *j* that is intercepted by a canopy element $\hat{a}$ inclined at angle $d\theta_r$ within layer *i*

D^i precipitation that drips from each canopy layer (m)

e_0 windless sensible heat correction factor (2.0 W/m^2)

f_{ik} leaf slope distribution functions

F_c sum of energy terms in the canopy

$g(i, \theta_r)$ mean layer projection in direction θ_r

H_c sensible heat at the air/canopy interface (W/m^2)

I^i intercepted precipitation by each layer (m)

$I_{ir}^{\downarrow}$ incoming infrared radiation (W/m^2)

$I_{ir,g}^{\downarrow}$ downwelling longwave flux at the ground (W/m^2)

$I_s^{\downarrow}$ incoming solar radiation (W/m^2)

$I_{s,g}^{\downarrow}$ total solar flux reaching the ground (W/m^2)

$K(\theta_r, \theta_k)$ kernel used to calculate mean layer projection

l latent heat (J/kg)

l_{evap} latent heat of evaporation (J/kg)

l_{sub} latent heat of sublimation (2.838×10^6 J/kg)

L_c latent heat at the air/canopy interface (W/m^2)

LAI^i leaf area index (area/area)

M^i Markov clumping factor (0–1)

P_c precipitation heat flux (W/m^2)

P_r precipitation rate at the top of the canopy (m/s)

P_r^i precipitation rate within the canopy (m/s)

$P_0(i,r)$ probability of gap for canopy layer i in direction $\hat{r}$

q_a^i mixing ratio of the air within the canopy

q_{ac}^i mixing ratio of the air at the air–canopy interface

$q_{c,sat}^i$ saturated canopy mixing ratio

$\hat{r}$ unit vector representing the orientation of the source

$\left(r_c^i\right)''$ foliage wetness characterization

Re^i canopy layer reflectance

RH relative humidity at the top of the canopy (%)

RH_c^i relative humidity within the canopy (%)

S_{ij} longwave transfer matrix between sink layer i and source layer j

SAI^i stem area index (area/area)

T_a air temperature at the top of the canopy (K)

T_a^i air temperature within the canopy (K)

T_{ac}^i air temperature at the air/canopy interface (K)

T_c^i canopy temperature (K)

T_p precipitation temperature (K)

Tr^i canopy layer transmittance

W_{ac}^i wind speed in the canopy (m/s)

W_{ijr} weighting coefficients for the flux contribution from source layer j to sink layer i for leaf distribution k for a source with a direction given by θ_r, ϕ_r and is expressed as the probability of gap when traversing a layer in direction $\hat{r}$

W' adjusted wind speed (W' = 2.0 m/s if W is below 2.0 m/s)

Z_c total height of canopy (m)

$Z_{1/2}^i$ distance from top of canopy to layer mid point (m)

EXECUTIVE SUMMARY

The one-dimensional dynamic state of the ground model FASST (Fast All-season Soil Strength) is a state of the ground model developed by Frankenstein and Koenig (2004) as part of the Army's Battlespace Terrain Reasoning and Awareness (BTRA) research program. The ability to predict the state of the ground is essential to both manned and unmanned vehicle mobility, and personnel movement, as well as determining sensor performance for both military and civilian activities. FASST calculates the ground's moisture content, ice content, temperature, and freeze–thaw profiles as well as soil strength and surface ice and snow accumulation or depletion. The fundamental operations of FASST are the calculation of an energy and water budget that quantify both the flow of heat and moisture within the soil and also the exchange of heat and moisture at all interfaces (ground–air or ground–snow; snow–air) using both meteorological and terrain data. FASST is designed to accommodate a range of users, from those who have intricate knowledge of their site to those who only know the site location. It allows for 22 different terrain materials, including asphalt, concrete, bed rock, permanent snow, and the USCS soil types. At a minimum, the only weather data required are the air temperatures.

Vegetation has the potential to alter the soil surface properties. This affects the operational capacity of infrared sensors that rely on the signal differences between the target and the background. Also, mobility calculations are based, in part, on soil moisture. Depending on the soil type, the change in moisture ascribable to vegetation could determine whether the situation is go or no-go.

In its original form, the only effects vegetation had on FASST were to change the surface albedo and emissivity. Recently, a two tier, multilayer vegetation algorithm was added. These can be implemented separately or together. Both alter the soil surface energy and moisture budgets. As a result of adding these models to FASST, the method discussed in the original documentation (Frankenstein and Koenig 2004) for solving the soil surface temperature is no longer the most suitable whether vegetation is present or not. The current method is discussed in Section 1.4 below.

In this report we will discuss the energy balance equations used to solve for the low vegetation, canopy and ground temperatures. In solving these equations, the effects of precipitation interception and soil moisture modification due to root-uptake are incorporated.

FASST VEGETATION MODELS

SUSAN FRANKENSTEIN AND GEORGE KOENIG

1 LOW VEGETATION MODEL—SHRUBS, CROPS, GRASS, ETC.

1.1 Introduction

The energy budget of a simple vegetation layer on a soil surface is modeled using a steady-state semi-infinite plane parallel model (Deardorff 1978, Balick et al. 1981b), which is described by the foliage emissivity ε_f and albedo α_f, a foliage height Z and the foliage fractional coverage σ_f. The vegetation model (in this section the terms foliage and vegetation are used interchangeably) consists of a single, homogeneous layer that is infinite in the x and y directions. It incorporates grasses, shrubs, marsh, tundra, and desert vegetation.

1.2 Vegetation–Atmosphere Energy Model

The sum of the energy terms F_f, consisting of the absorbed solar and infrared fluxes, the emitted longwave flux, and the sensible heat, latent heat, and precipitation heat fluxes, is equal to zero at each time increment. The solution of the resulting polynomial equation of degree n, for the foliage temperature T_f (K) is obtained using a root-finding algorithm. The atmosphere–foliage energy exchange is given as

$$F_f = 0 = \sigma_f \left[I_s^{\downarrow}(1-\alpha_f) + \varepsilon_f I_{ir}^{\downarrow} - \varepsilon_f \sigma T_f^4 - P_f \right] + \frac{\sigma_f \varepsilon_f \varepsilon_g \sigma}{\varepsilon_l}(T_g^4 - T_f^4) + H_f + L_f \tag{1}$$

where

T_g = ground temperature (K)

ε_g = ground emissivity

σ = Stefan-Boltzman constant (5.699×10^{-8} W/m^2·K^4)

$I_s^{\downarrow}$ = total incoming solar radiation (W/m^2)

$I_{ir}^{\downarrow}$ = total incoming infrared radiation (W/m^2)

H_f = sensible heat flux (W/m^2)

L_f = latent heat flux (W/m^2)

P_f = precipitation heat flux (W/m^2)

and ε_l is defined in equation 6. The foliage fractional coverage σ_f and the short-wave albedo α_f are functions of the vegetation type (high, medium, or low) and the season (winter, spring, summer, and fall). Default values are listed in Appendix A. If the foliage fraction is not known, it is calculated using the method developed by Ramírez and Senarath (2000) and is defined as

$$\sigma_f = 1 - \exp(-0.75LAI) \quad \text{grasses}$$

$$\sigma_f = \begin{cases} \sigma_{f,max} & T_g > 298.0 \\ \sigma_{f,min} & T_g < 273.15 \\ \sigma_{f,max} - \left[1 - F\left(T_g\right)\right]\left[\sigma_{f,max} - \sigma_{f,min}\right] & 273.15 \le T_g \le 298.0 \end{cases} \quad \text{other vegetation} \tag{2}$$

where

$$LAI = LAI_{min} + F\left(T_g\right)\left[LAI_{max} - LAI_{min}\right]$$
$$F\left(T_g\right) = 1.0 - 0.0016\left[298.0 - T_g\right]^2 \tag{3}$$

The values for LAI_{min}, LAI_{max}, $\sigma_{f,max}$, and $\sigma_{f,min}$ are given in Table 1. Also given in Table 1 is *SAI*, the stem area index. The term *LAI* in eq 3 is the leaf area index for the vegetation. *LAI* is defined as the total one-sided leaf (vegetation) area occupying the horizontally projected area of the vegetation. The *LAI* is an indication of the vegetation overlap and is dependent on the temperature of the vegetation (eq 3) as parameterized by Ramírez and Senarath (2000).

Table 1. Low vegetation properties.

Biome	high/ medium/ low	$\sigma_{f,max}$* (%)	$\sigma_{f,min}$* (%)	LAI_{max}* (m^2/m^2)	LAI_{min}* (m^2/m^2)	SIA* (m^2/m^2)
crop	m	85	25	6.0	0.5	0.5
short grass	l	80	70	2.0	0.5	4.0
tall grass	m	80	50	6.0	0.5	2.0
desert	l	5	0	2.0	0	0.5
tundra	m	60	40	6.0	0.5	0.5
irrigated crops	m	80	20	6.0	0.5	0.5
semidesert	m	10	0	6.0	0.5	2.0
bog/marsh	l	80	40	6.0	0.5	2.0
evergreen shrub	h	80	60	6.0	5.0	2.0
deciduous shrub	h	80	50	6.0	1.0	2.0

* Dickinson et al. (1986)

1.2.1 Solar and Infrared Radiation

The first term $\sigma_f I_s^{\downarrow}(1-\alpha_f)$ on the right-hand side of eq 1 is the total solar flux $I_s^{\downarrow}$ absorbed by the vegetation. The vegetation reflected solar flux is given by $\sigma_f I_s^{\downarrow}\alpha_f$ and the solar flux transmitted through the vegetation to the underlying soil is given as $I_s^{\downarrow}(1-\sigma_f)$. The total solar flux is one of the meteorological parameters required to run the models. The vegetation absorbed atmospheric downwelling longwave flux is given as $\varepsilon_f\sigma_f I_{ir}^{\downarrow}$. The vegetation longwave emissivity, ε_f, is a function of the vegetation type and the season. It is assumed that the foliage longwave emissivity ε_f is equal to the foliage longwave absorptivity, a_f^{ir}. The maximum value of ε_f in the model is 0.96 and the minimum is 0.90. It varies linearly between the two values according to $\varepsilon_f = 0.90 + F\left(T_g\right)[0.96-0.90]$ where $F\left(T_g\right)$ is given in eq 3. $I_{ir}^{\downarrow}$ is obtained from the meteorological database. The vegetation emitted longwave flux is given as $\sigma_f\varepsilon_f\sigma T_f^4$ where σ is the Stefan-Boltzmann constant and T_f, the vegetation temperature, is the variable for which the equation is being solved. The term given as

$$\frac{\sigma_f\varepsilon_f\varepsilon_g\sigma}{\varepsilon_l}(T_g^4 - T_f^4)$$

in eq 1 is the radiative exchange between the ground and the vegetation and is obtained by applying the adding method of radiative transfer to two layers including multiple reflections as outlined in Figure 1.

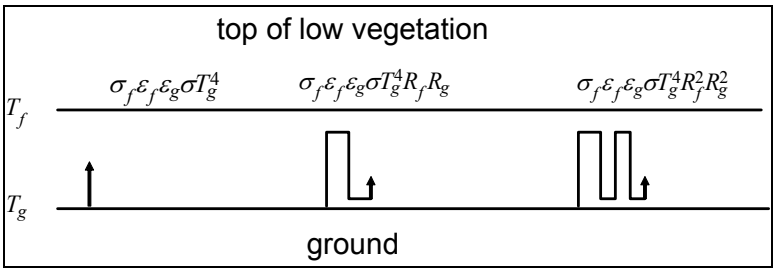

Figure 1. Adding method of radiative transfer to two layers including multiple reflections.

If the longwave emissivity is assumed to equal the longwave absorptivity and foliage reflectance is defined as $R_f = (1 - \varepsilon_f)$ and ground reflectance as $R_g = (1 - \varepsilon_g)$, the ground-emitted longwave flux absorbed by the vegetation, including multiple reflections, is given as (sum the terms indicated in the above figure)

$$\sigma_f \varepsilon_f \varepsilon_g \sigma T_g^4 (1 + R_f R_g + R_f^2 R_g^2 + \cdots)$$

and σ_f accounts for the vegetation density. As $R_g \leq 1$, $R_f \leq 1$ the series can be approximated and the absorbed flux is given as

$$\sigma_f \varepsilon_f \varepsilon_g \sigma T_g^4 (1 - R_f R_g)^{-1} \tag{4}$$

The vegetation-emitted flux, $\sigma_f \varepsilon_f \sigma T_f^4$, and the vegetation-emitted flux that is absorbed by the vegetation, $\sigma_f \varepsilon_f^2 \sigma T_f^4 R_g + \cdots$, including multiple reflections, are depicted in Figure 2.

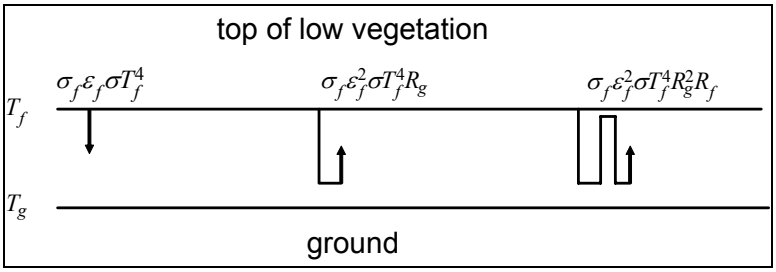

Figure 2. Vegetation-emitted flux, and the vegetation-emitted flux that is absorbed by the vegetation, including multiple reflections.

Summing the terms gives

$$\sigma_f \varepsilon_f^2 \sigma T_f^4 R_g (1 + R_g R_f + R_g^2 R_f^2 + \cdots) - \sigma_f \varepsilon_f \sigma T_f^4$$

and approximating the series as before gives

$$\frac{\sigma_f \varepsilon_f^2 \sigma T_f^4 R_g}{1 - R_f R_g} - \sigma_f \varepsilon_f \sigma T_f^4$$

with a little algebraic manipulation, this expression reduces to

$$-\frac{\sigma_f \varepsilon_f \varepsilon_g \sigma T_f^4}{1 - R_f R_g} \tag{5}$$

The total longwave flux emitted and absorbed by the vegetation (sum eq 4 and 5 using the definition for R_f and R_g) is

$$\frac{\sigma_f \varepsilon_f \varepsilon_g \sigma}{\varepsilon_l} (T_g^4 - T_f^4); \quad \varepsilon_l = \varepsilon_f + \varepsilon_g - \varepsilon_f \varepsilon_g \tag{6}$$

The ground emissivity ε_g is a function of the soil type and ranges from 0.92 to 0.97.

1.2.2 Sensible Heat Flux

The sensible flux between the vegetation and the air surrounding the vegetation is given as (Deardorff 1978)

$$H_f = \left(e_0 + 1.1LAI\rho_{af}c_{p,a}C_f W_{af}\right)(T_{af} - T_f) \tag{7}$$

where

e_0 = windless exchange coefficient for sensible heat (2.0 W/m^2) (Jordan 1996)

C_f = bulk transfer coefficient

T_{af} = air temperature in the foliage (K)

W_{af} = wind speed at the air/foliage interface (m/s)

$c_{p,a}$ = specific heat of air at constant pressure (1005.6 J/kg·K).

The air density in the foliage ρ_{af} (kg/m^3) near the atmosphere–foliage interface is given as

$$\rho_{af} = \frac{\rho_a + \rho_f}{2} \tag{8}$$

where the densities ρ_a and ρ_f (kg/m^3) are calculated using the ideal gas law ($P_a = \rho RT$), R is the gas constant for air, and P_a (Pa) is the measured atmospheric pressure). For ρ_a, $T = T_a$ (K) the air temperature measured at the shelter height Z_a (m), and for ρ_f, $T = T_f$. For the first time step, T_f is set equal to 0.9 T_a in order to calculate ρ_f. Air temperature in the foliage (T_{af}) is modeled as (Deardorff 1978)

$$T_{af} = (1 - \sigma_f)T_a + \sigma_f(0.3T_a + 0.6T_f + 0.1T_g) \tag{9}$$

Following Deardorff (1978), the bulk transfer coefficient, C_f, is

$$C_f = 0.01(1 + 0.3/W_{af}) \tag{10}$$

The wind speed in the foliage is given as

$$W_{af} = 0.83\sigma_f W'\sqrt{C_{hn}^f} + (1 - \sigma_f)W' \tag{11}$$

where W' = 2.0 m/s if W is below 2.0 m/s, otherwise it is set to the ambient wind speed (Kahle 1977, Hughes et al. 1993). The bulk transfer coefficient C_{hn}^f at the top of the foliage is indicative of the transfer of momentum between the atmos-

phere and the foliage. For conditions of near-neutral stability C_{hn}^{f} is calculated using

$$C_{hn}^{f} = \left[k / \ln\left(\frac{Z_a - Z_d}{z_0^f} \right) \right]^2 \tag{12}$$

The roughness length z_0^f (m) is defined as the height where the mean speed, $\overline{u(z)}$ (m/s), goes to zero. Default values for the different vegetation types are given in Table 2. $\overline{u(z)}$ is given as

$$\overline{u(z)} = \frac{u_*}{k} \ln\left(\frac{Z_a}{z_0^f} \right) \tag{13}$$

$u_*$is a friction velocity (m/s) and k is von Karmen's constant (k = 0.4). When foliage is present, the height at which the logarithmic wind profile goes to zero is displaced upward by an amount defined as the zero displacement height Z_d (m). The zero displacement height and the foliage roughness length are calculated from (Balick et al. 1981b)

$$\begin{aligned} Z_d &= 0.701 Z_f^{0.975} \\ z_0^f &= 0.131 Z_f^{0.997} \end{aligned} \tag{14}$$

Z_f (m), the vegetation height, is a function of the vegetation type (low, middle, and high) and season, and is hardwired in the code. Default values are listed in Appendix A. If $z_0^f < 0.02$ m, then the default value found in Table 2 is used.

Table 2. Additional low vegetation properties.

Biome	$r_{s,min}$* (s/m)	z_0^f* (m)	g_D† (10^{-2} Pa^{-1})	d_{max}** (mm)	a_r† (m^{-1})	b_r† (m^{-1})
crop	120	0.06	0.0	0.20	5.558	2.614
short grass	200	0.02	0.0	0.20	10.739	2.608
tall grass	200	0.10	0.0	0.20	8.235	1.627
desert	200	0.05	0.0	0.20	4.372	0.978
tundra	200	0.04	0.0	0.20	8.992	8.992
irrigated crops	200	0.06	0.0	0.20	5.558	2.614
Semidesert	200	0.10	0.0	0.20	4.372	0.978
bog/marsh	200	0.03	0.0	0.20	7.344	1.303
evergreen shrub	200	0.10	0.0	0.25	6.326	1.567
deciduous shrub	200	0.10	0.0	0.10	6.326	1.567

* Dickinson et al. (1986)
† http://www.ecmwf.int/research/ifsdocs/CY25r1/Physics/Physics-08-03.html
** Ramírez and Senarath (2000)

1.2.3 Latent Heat Flux

The latent heat flux exchange between the foliage and the surrounding atmosphere is given as (Deardorff 1978)

$$L_f = LAI\rho_{af}C_f l W_{af} r''(q_{af} - q_{f,\,sat}) \tag{15}$$

where l is either the latent heat of evaporation, l_{evap}, or sublimation, l_{sub} (2.838×10^6 J/kg), depending on the air and surface temperatures; C_f, W_{af}, and ρ_{af} are calculated as before, q_{af} is the mixing ratio of the air at the foliage interface, and $q_{f,\,sat}$ is the saturated foliage mixing ratio. Balick et al. (1981a) give the latent heat of evaporation as

$$l_{evap} = 2{,}500{,}775.6 - 2369.729\left[\frac{T_a - T_g}{2} - 273.15\right] \tag{16}$$

r" represents the foliage surface wetness and is a function of the air and stomatal resistance to vapor diffusion. It is given as

$$r'' = \frac{r_a}{r_a + r_s} \tag{17}$$

where the atmospheric resistance to water vapor diffusion r_a is given as

$$r_a = 1/C_f W_{af} \tag{18}$$

The vegetation stomatal resistance to vapor diffusion, r_s, is parameterized as (Chen et al. 1996, ECMWF 2002)

$$\begin{gathered} r_s = \frac{r_{s,\min}}{LAI} f_1 f_2 f_3 \\ \frac{1}{f_1} = \min\left[1, \frac{0.004 I_s^{\downarrow} + 0.005}{0.81\left(0.004 I_s^{\downarrow} + 1\right)}\right] \\ \frac{1}{f_2} = \begin{cases} 0 & \theta_r > \overline{\theta} \; or \; \overline{\theta} > \theta_{max} \\ \dfrac{\overline{\theta} - \theta_r}{\theta_{max} - \theta_r} & \theta_r \le \overline{\theta} \le \theta_{max} \end{cases} \\ \frac{1}{f_3} = \exp\left(-g_D\left[e_{f,sat} - e_a\right]\right) \end{gathered} \tag{19}$$

where θ_r, θ_{max} are the residual and maximum soil moisture contents (m^3/m^3) respectively, $e_{f,sat}$, e_a (Pa) the saturated foliage and air vapor pressures, respectively, are described further below and $\overline{\theta}$, the average root soil water, is

$$\begin{gathered} \overline{\theta} = \sum_{p=1}^{nodes} R_p \theta_p \\ R_p = 0.5\left[\exp\left(-a_r z_{p-1/2}\right) + \exp\left(-b_r z_{p-1/2}\right) - \exp\left(-a_r z_{p+1/2}\right) - \exp\left(-b_r z_{p+1/2}\right)\right] \end{gathered} \tag{20}$$

R_p represents the fraction of roots at node p and θ_p is the soil moisture at node p, both located at a depth of z_p. The values of g_D, a_r and b_r for the different vegetation types are given in Table 2. During periods of full solar loading the stomatal resistance is low, resulting in an increase in the latent heat exchange, while at night it is high ($I_s^{\downarrow} = 0$ and $f_1 = 162$). In dry areas like Yuma, Arizona, when there is little or no available soil moisture, r_s will be very large ($f_2 \to \infty$) and $L_f \to 0$.

Balick et al. (1981b) quantify the mixing ratios as

$$q_{\mathrm{a}} = \frac{0.622 e_{\mathrm{a}}}{P_{\mathrm{a}} - e_{\mathrm{a}}} \tag{21}$$

where e_{a} is the vapor pressure (Pa) calculated from the algorithm of Buck (1981) as

$$e_{\mathrm{a}} = e_{\mathrm{a}}^{0} RH \exp\left[a(T_{\mathrm{a}} - 273.16)/(T_{\mathrm{a}} - b)\right] \tag{22}$$

where $e_{\mathrm{a}}^{0} (= 610.78 \text{ Pa})$ is the saturation vapor pressure at 0°C and

$$a = \begin{cases} 17.269 & \text{over water} \\ 21.8745 & \text{over ice/snow} \end{cases}$$

$$b = \begin{cases} 35.86 \text{ K} & \text{over water} \\ 7.66 \text{ K} & \text{over ice/snow} \end{cases}$$

The mixing ratio of the air in the foliage is (Deardorff 1978, Balick et al. 1981b)

$$q_{\mathrm{af}} = \frac{[(1 - \sigma_{\mathrm{f}}) q_{\mathrm{a}} + \sigma_{\mathrm{f}} (0.3 q_{\mathrm{a}} + 0.6 q_{\mathrm{f,\,sat}} r'' + 0.1 q_{\mathrm{g,\,sat}} M_{\mathrm{g}})]}{1 - \sigma_{\mathrm{f}} [0.6(1 - r'') + 0.1\left(1 - M_{\mathrm{g}}\right)]} \tag{23}$$

where $q_{\mathrm{f,\,sat}}$ and $q_{\mathrm{g,\,sat}}$ (saturated ground mixing ratio) are given in eq 21 and 22 with the subscripts *f* and *g* replacing *a* and $RH = 1$ (100%) and M_g is the ground moisture factor ($0 \le M_{\mathrm{g}} \le 1$). A detailed discussion of the calculation of M_g is found in Frankenstein and Koenig (2004).

1.2.4 Precipitation Heat Flux

Following the method of Jordan (1991) gives the precipitation heat flux for a bare surface as

$$\begin{aligned} P &= U_{\mathrm{p}} c_{\mathrm{p}} T_{\mathrm{p}} \\ U_{\mathrm{p}} &= -\gamma_{\mathrm{p}} \cdot \text{fall rate} \end{aligned} \tag{24}$$

with T_p the precipitation temperature defined as the air wet-bulb temperature, c_p either the specific heat of water, $c_{p,w}$ (4217.7 J/kg·K) or ice, $c_{p,i}$ (–13.3 + 7.80T_a J/kg·K) depending on T_p, U_p the mass precipitation flux (kg/m^2·s) and γ_p the precipitation density (kg/m^3). The fall rate is in meters per second. Equation 24 assumes that all of the precipitation that falls makes contact with the ground. If vegetation is present, some of this will be intercepted. Of the intercepted precipitation (I), some will be stored (S_c), evaporated (E_f), transpired (E_{tr}), or dripped (D) such that the amount of moisture on the surface of the vegetation is (Deardorff 1978, Sellers et al. 1986)

$$S_c = \left(I - D - \left(E_f - E_{tr}\right)\right)\Delta t \tag{25}$$

where (Dai et al. 2001, Deardorff 1978)

$$\begin{aligned}
I &= \left[1.0 - \exp\left\{-0.5\left(LAI + SAI\right)\right\}\right]\sigma_f P_r \\
D &= \begin{cases} \dfrac{S_c - S_{c,\,max}}{\Delta t} & S_c > S_{c,\,max} \\ 0 & \text{otherwise} \end{cases} \\
E_f &= \left(1 - \delta_c\left[\frac{r_s}{r_a + r_s}\right]\left[1 - \left(\frac{S_c}{S_{c,\,max}}\right)^{2/3}\right]\right)E_p \\
E_{tr} &= \delta_c\left[\frac{r_a}{r_a + r_s}\right]\left[1 - \left(\frac{S_c}{S_{c,\,max}}\right)^{2/3}\right]E_p
\end{aligned} \tag{26}$$

and (Ramírez and Senarath 2000, Deardorff 1978)

$$\begin{aligned}
S_{c,\,max} &= 1000 d_{max}\left(LAI + SAI\right) \\
E_p &= LAI\,\rho_a C_f W_{af}\left[q_{af} - q_{f,\,sat}\right]
\end{aligned} \tag{27}$$

where

δ_c = 0 if $q_{f,\,sat} > q_{af}$ else $\delta_c = 1$

P_r = precipitation rate (m/s) (fall rate in eq 24)

SAI = stem area index (m^2/m^2) (Table 1)

$S_{c,\,max}$ = maximum storage capacity (m)

Δt = time step (s)

E_p = potential evaporation (m/s)

d_{max} = maximum dew depth (mm) (Table 2)

$q_{f,\,sat}$, = saturated foliage mixing ratio

q_{af} = foliage/atmosphere mixing ratio.

The transpiration rate is limited by the amount of water that the roots can uptake (Dickinson et al. 1986)

$$E_{tr,\,max} = 1.5 \times 10^{-7} \sigma_f ff \sum_{k=1}^{nnodes} R_k \left[1 - \frac{\theta_k - \theta_r}{\theta_{max} - \theta_r} \right] \tag{28}$$

$ff = 1$ if the soil is unfrozen or else $ff = 0$ and the other terms are as described previously. If $E_{tr} > E_{tr,\,max}$, then $E_{tr} = E_{tr,\,max}$ and eq 26 is rearranged and solved for r_s before recalculating E_f, the foliage evaporation rate. Putting all of this together gives the foliage precipitation heat flux as

$$P_f = -\gamma_p \left[1.0 - \exp\left\{ -0.5\left(LAI + SAI \right) \right\} \right] P_r c_p T_p \tag{29}$$

1.2.5 Final Foliage–Atmosphere Energy Equation

Combining eq 1, 7, 15, and 29 gives the final foliage/atmosphere energy equation

$$\begin{aligned} F_f = 0 = {} & \sigma_f \left[I_s^{\downarrow} (1 - \alpha_f) + \varepsilon_f I_{ir}^{\downarrow} - \varepsilon_f \sigma T_f^4 - \gamma_p \left[1.0 - \exp\left\{ -0.5\left(LAI + SAI \right) \right\} \right] P_r c_p T_p \right] \\ & + \frac{\sigma_f \varepsilon_f \varepsilon_g \sigma}{\varepsilon_l} (T_g^4 - T_f^4) + \left(e_0 + 1.1 LAI \rho_{af} c_{p,a} C_f W_{af} \right) (T_{af} - T_f) \\ & + LAI \rho_{af} C_f l W_{af} r'' (q_{af} - q_{f,\,sat}) \end{aligned} \tag{30}$$

1.3 Foliage–Ground Energy Model

The equation for F_f (eq 30) contains two unknowns: T_f and T_g. To solve for these quantities, it is necessary to formulate another equation containing at least

one of the unknown variables. This can be done by formulating the energy flux exchange at the foliage–ground interface as

$$F(T_g) = 0 = (1-\sigma_f)\left[I_s^{\downarrow}(1-\alpha_g) + \varepsilon_g I_{ir}^{\downarrow} - \varepsilon_g \sigma T_g^4\right] - P_g - \frac{\sigma_f \varepsilon_f \varepsilon_g \sigma}{\varepsilon_l}(T_g^4 - T_f^4) + H_g + L_g + \kappa\frac{\partial T_g}{\partial z} + l_{fus}\frac{\rho_i}{\rho_w}\frac{\partial \theta_k}{\partial t}\Delta z - v c_p T_g \quad (31)$$

where

$(1 - \sigma_f)$ = radiant and precipitation fluxes not intercepted by the vegetation

α_g = shortwave albedo of the ground

κ = is the soil thermal conductivity at the surface (W/m·K)

l_{fus} = latent heat of fusion (J/kg)

ρ_i = density of ice (kg/m^3)

ρ_w = density of water (kg/m^3)

θ_k = change in volumetric ice content at the surface

v = amount of water flowing towards/away from the surface (m/s).

Both α_g and ε_g are functions of the soil type and range from 0.23 to 0.40 and 0.92 to 0.97, respectively. The third term in the second row of eq 31 takes care of heat conduction to and from the surface by the underlying ground, depending on the temperature gradient. This is followed by the heat released and absorbed by the soil as the soil moisture melts or freezes. Finally, the last term represents heat that is advected away from or towards the surface owing to the vertical movement of moisture. The radiant physical processes are the same as those given earlier but for the foliage–ground interface rather than the atmosphere–foliage interface.

1.3.1 Sensible Heat Flux

The sensible heat exchange is given as

$$H_g = \left(e_0 + \rho_{ag} c_{p,a} C_h^g W_{af}\right)(T_{af} - T_g) \quad (32)$$

where the air density ρ_{ag} (kg/m^3) near the foliage–ground interface is calculated using the ideal gas law, the atmospheric pressure, and the air temperature in the

foliage T_{af} near the ground. The bulk transfer coefficient for sensible heat C_h^g is calculated using the bulk transfer coefficient near the ground C_{hn}^g and at the atmosphere–foliage interface C_{hn}^f, as previously defined (eq 12) for near neutral stability plus a sensible heat exchange stability correction factor Γ_h

$$C_h^g = \Gamma_h[(1-\sigma_f)C_{hn}^g + \sigma_f C_{hn}^f]$$

$$C_{hn}^g = \frac{\left[\dfrac{k}{\ln\left(Z_a / z_o^g\right)}\right]^2}{\left[r_{ch} + \dfrac{\ln(Z_a/Z_u)}{\ln(Z_a/z_o^g)}\right]} \tag{33}$$

The ground roughness length z_o^g (m) is equal to 0.001 m for all soil types and 0.0006 m for snow. Because Z_a (m), the height of the measured air temperature, equals Z_u (m), the height of the measured wind speed, C_{hn}^g reduces to

$$C_{hn}^g = \frac{\left[\dfrac{k}{\ln\left(Z_a / z_o^g\right)}\right]^2}{r_{ch}} \tag{34}$$

where the turbulent Schmidt number r_{ch} is hardwired in the code as 0.63 for all soil types. The term Γ_h in eq 33 accounts for non-neutral conditions and is defined as

$$\Gamma_h = \begin{cases} \dfrac{1.0}{\left(1.0 - 16.0 R_{ib}\right)^{0.5}} & R_{ib} < 0.0 \\ 1.0 & R_{ib} = 0.0 \\ \dfrac{1.0}{1.0 - 5.0 R_{ib}} & 0.0 < R_{ib} < 0.2 \end{cases} \tag{35}$$

$$R_{ib} = \frac{2gZ_a\left(T_{af} - T_g\right)}{\left(T_{af} + T_g\right)W_{af}^2}$$

where R_{ib} is the bulk Richardson number and g is the gravitational constant (9.81 m/s^2). It is evident from the equation for the bulk Richardson number that its sign depends on the temperature of the ground relative to the air temperature. For a

specific air ground temperature difference, an increase in the wind speed will reduce the absolute value of the bulk Richardson number. For relatively calm conditions, when the ground is colder than the air, the air near the ground will be cooled and the atmosphere will be stable, resulting in a decrease in the air–ground temperature difference and a reduction in the sensible heat flux. If the ground is warmer than the air, the air will be heated and an unstable atmospheric condition can develop.

1.3.2 Latent Heat Flux

The latent heat exchange at the foliage–ground interface is given as

$$L_g = C_e^g l W_{af} \rho_{ag} (q_{af} - q_g) \tag{36}$$

and

$$C_e^g = \Gamma_e [(1 - \sigma_f) C_{en}^g + \sigma_f C_{hn}^f] \tag{37}$$

$\Gamma_e = \Gamma_h$ and C_{en}^g follows the development for C_{hn}^g with Z_a being replaced with Z_{rh} (m), the height above the ground of the relative humidity measurement, and r_{ch} with r_{ce} the turbulent Prandtl number (0.71, hardwired in the code). l is either the latent heat of evaporation, l_{evap} given in eq 16 or sublimation, l_{sub} (2.838×10^6 J/kg), depending on the air and surface temperatures.

In eq 36 q_g is the mixing ratio of the air at the surface and q_{af} is the mixing ratio of the air at the foliage interface. The mixing ratio $q_g = M_g q_{g,\,sat}(T_g) + (1–M_g) q_{af}$ with M_g being the moisture factor ($0 \le M_g \le 1$) and $q_{g,sat}$ the saturated mixing ratio. The value assigned to the moisture factor depends on the degree of saturation of the soil. If it is raining, $M_g = 1$, otherwise, it is equal to the surface soil moisture content (Frankenstein and Koenig 2004).

1.3.3 Precipitation Heat Flux

The amount of precipitation striking the ground is

$$P_{r,g} = P_r - I + D \tag{38}$$

where P_r is the precipitation rate, I is the amount intercepted by the foliage, and D is the amount that drips from the foliage if the moisture on the leaf surface ex-

ceeds its storage capacity. I and D are defined in eq 26. Substituting eq 38 into eq 24, the ground precipitation heat flux (P_g) is

$$P_{\mathrm{g}} = -\gamma_{\mathrm{p}}\left(P_{\mathrm{r}} - I + D\right)c_{\mathrm{p}}T_{\mathrm{p}} \tag{39}$$

1.3.4 Final Foliage–Ground Energy Equation

Combing eq 31, 32, 36, and 39 gives the final foliage/ground energy equation

$$\begin{aligned} F(T_{\mathrm{g}}) = 0 = {} & \left(1-\sigma_{\mathrm{f}}\right)\left[I_{\mathrm{s}}^{\downarrow}(1-\alpha_{\mathrm{g}}) + \varepsilon_{\mathrm{g}} I_{\mathrm{ir}}^{\downarrow} - \varepsilon_{\mathrm{g}}\sigma T_{\mathrm{g}}^4\right] + \gamma_{\mathrm{p}}\left(P_{\mathrm{r}} - I + D\right)c_{\mathrm{p}}T_{\mathrm{p}} \\ & - \frac{\sigma_{\mathrm{f}}\varepsilon_{\mathrm{f}}\varepsilon_{\mathrm{g}}\sigma}{\varepsilon_1}(T_{\mathrm{g}}^4 - T_{\mathrm{f}}^4) + \left(e_0 + \rho_{\mathrm{ag}}c_{\mathrm{p,a}}C_{\mathrm{h}}^{\mathrm{g}}W_{\mathrm{af}}\right)(T_{\mathrm{af}} - T_{\mathrm{g}}) \\ & + C_{\mathrm{e}}^{\mathrm{g}} l W_{\mathrm{af}}\rho_{\mathrm{ag}}M_{\mathrm{g}}(q_{\mathrm{af}} - q_{\mathrm{g,\,sat}}) + \kappa\frac{\partial T_{\mathrm{g}}}{\partial z} + l_{\mathrm{fus}}\frac{\rho_{\mathrm{i}}}{\rho_{\mathrm{w}}}\frac{\partial\theta_{\mathrm{i}}}{\partial t}\Delta z - vc_{\mathrm{p}}T_{\mathrm{g}} \end{aligned} \tag{40}$$

1.4 Numerical Solution

In order to solve eq 30 and 40, it is assumed that

$$\begin{aligned} \kappa\frac{\partial T_{\mathrm{g}}}{\partial z} &= \kappa\frac{(T_2 - T_{\mathrm{g}})}{\Delta z} \\ T_{\mathrm{g}}^4 &= \left(T_{\mathrm{g}}\right)_{\mathrm{m-1}}^4 + 4\left(T_{\mathrm{g}}\right)_{\mathrm{m-1}}^3\left[T_{\mathrm{g}} - \left(T_{\mathrm{g}}\right)_{\mathrm{m-1}}\right] \\ q_{\mathrm{g,\,sat}} &= q_{\mathrm{g,\,sat}}\left(\left(T_{\mathrm{g}}\right)_{\mathrm{m-1}}\right) + \left.\frac{\partial q_{\mathrm{g,\,sat}}}{\partial T_{\mathrm{g}}}\right|_{T_{\mathrm{g}}=\left(T_{\mathrm{g}}\right)_{\mathrm{m-1}}}\left[T_{\mathrm{g}} - \left(T_{\mathrm{g}}\right)_{\mathrm{m-1}}\right] \end{aligned} \tag{41}$$

where T_2 is the temperature just below the surface and the subscript $m - 1$ indicates the values of T_{g} at the previous time step. T_{f}^4 and $q_{\mathrm{f,\,sat}}$ are also represented by eq 41, substituting the subscript g with f. The above substitutions allow the linearization of eq 30 and 40, which can then be solved simultaneously for T_{f} and T_{g}. The final equations are thus

$$\begin{aligned} c_1^{\mathrm{f}} + c_2^{\mathrm{f}}T_{\mathrm{g}} + c_3^{\mathrm{f}}T_{\mathrm{f}} &= 0 \\ c_1^{\mathrm{g}} + c_2^{\mathrm{g}}T_{\mathrm{g}} + c_3^{\mathrm{g}}T_{\mathrm{f}} &= 0 \end{aligned} \tag{42}$$

where

$$
\begin{aligned}
c_1^{\mathrm{f}} &= \sigma_{\mathrm{f}}\left[I_{\mathrm{s}}^{\downarrow}(1-\alpha_{\mathrm{f}}) + \varepsilon_{\mathrm{f}} I_{\mathrm{ir}}^{\downarrow} - \gamma_{\mathrm{p}}\left[1.0 - \exp\left\{-0.5\left(LAI + SAI\right)\right\}\right] P_{\mathrm{r}} c_{\mathrm{p}} T_{\mathrm{p}} \right] \\
&\quad - 3\frac{\sigma_{\mathrm{f}}\varepsilon_{\mathrm{f}}\varepsilon_{\mathrm{g}}\sigma}{\varepsilon_1}\left(T_{\mathrm{g}}\right)_{\mathrm{m-1}}^4 - 3\left[-\sigma_{\mathrm{f}}\varepsilon_{\mathrm{f}}\sigma - \frac{\sigma_{\mathrm{f}}\varepsilon_{\mathrm{f}}\varepsilon_{\mathrm{g}}\sigma}{\varepsilon_1}\right]\left(T_{\mathrm{f}}\right)_{\mathrm{m-1}}^4 \\
&\quad + sheatf\left(1-0.7\sigma_{\mathrm{f}}\right)T_{\mathrm{a}} + LAI\rho_{\mathrm{af}}C_{\mathrm{f}}lW_{\mathrm{af}}r''\left(\frac{1-0.7\sigma_{\mathrm{f}}}{d_1}\right)q_{\mathrm{a}} \\
&\quad + LAI\rho_{\mathrm{af}}C_{\mathrm{f}}lW_{\mathrm{af}}r''\left(\frac{0.6\sigma_{\mathrm{f}}r''}{d_1} - 1\right)\left[q_{\mathrm{f,\,sat}}\left(\left(T_{\mathrm{f}}\right)_{\mathrm{m-1}}\right) - \left(T_{\mathrm{f}}\right)_{\mathrm{m-1}}\left.\frac{\partial q_{\mathrm{f,\,sat}}}{\partial T_{\mathrm{f}}}\right|_{T_{\mathrm{f}}=\left(T_{\mathrm{f}}\right)_{\mathrm{m-1}}} \right] \\
&\quad + LAI\rho_{\mathrm{af}}C_{\mathrm{f}}lW_{\mathrm{af}}r''\left(\frac{0.1\sigma_{\mathrm{f}}M_{\mathrm{g}}}{d_1}\right)\left[q_{\mathrm{g,\,sat}}\left(\left(T_{\mathrm{g}}\right)_{\mathrm{m-1}}\right) - \left(T_{\mathrm{g}}\right)_{\mathrm{m-1}}\left.\frac{\partial q_{\mathrm{g,\,sat}}}{\partial T_{\mathrm{g}}}\right|_{T_{\mathrm{g}}=\left(T_{\mathrm{g}}\right)_{\mathrm{m-1}}} \right] \\
c_2^{\mathrm{f}} &= 4\frac{\sigma_{\mathrm{f}}\varepsilon_{\mathrm{f}}\varepsilon_{\mathrm{g}}\sigma}{\varepsilon_1}\left(T_{\mathrm{g}}\right)_{\mathrm{m-1}}^3 + 0.1\sigma_{\mathrm{f}}sheatf \\
&\quad + LAI\rho_{\mathrm{af}}C_{\mathrm{f}}lW_{\mathrm{af}}r''\left(\frac{0.1\sigma_{\mathrm{f}}M_{\mathrm{g}}}{d_1}\right)\left.\frac{\partial q_{\mathrm{g,\,sat}}}{\partial T_{\mathrm{g}}}\right|_{T_{\mathrm{g}}=\left(T_{\mathrm{g}}\right)_{\mathrm{m-1}}} \\
c_3^{\mathrm{f}} &= 4\left[-\sigma_{\mathrm{f}}\varepsilon_{\mathrm{f}}\sigma - \frac{\sigma_{\mathrm{f}}\varepsilon_{\mathrm{f}}\varepsilon_{\mathrm{g}}\sigma}{\varepsilon_1}\right]\left(T_{\mathrm{f}}\right)_{\mathrm{m-1}}^3 + \left(0.6\sigma_{\mathrm{f}} - 1\right)sheatf \\
&\quad + LAI\rho_{\mathrm{af}}C_{\mathrm{f}}lW_{\mathrm{af}}r''\left(\frac{0.6\sigma_{\mathrm{f}}r''}{d_1} - 1\right)\left.\frac{\partial q_{\mathrm{f,\,sat}}}{\partial T_{\mathrm{f}}}\right|_{T_{\mathrm{f}}=\left(T_{\mathrm{f}}\right)_{\mathrm{m-1}}}
\end{aligned}
\tag{43}
$$

$$
\begin{aligned}
c_1^{\mathrm{g}} &= \left(1-\sigma_{\mathrm{f}}\right)\left[I_{\mathrm{s}}^{\downarrow}(1-\alpha_{\mathrm{g}})+\varepsilon_{\mathrm{g}} I_{\mathrm{ir}}^{\downarrow}\right]+\gamma_{\mathrm{p}}\left(P_{\mathrm{r}}-I+D\right)c_{\mathrm{p}}T_{\mathrm{p}}+\frac{\kappa_1}{\Delta z_1}T_2+l_{\mathrm{fus}}\frac{\rho_{\mathrm{i}}}{\rho_{\mathrm{w}}}\frac{\partial\theta_{\mathrm{i}}}{\partial t}\Delta z_1 \\
&\quad -3\frac{\sigma_{\mathrm{f}}\varepsilon_{\mathrm{f}}\varepsilon_{\mathrm{g}}\sigma}{\varepsilon_1}\left(T_{\mathrm{f}}\right)_{\mathrm{m-1}}^4-3\left[-\left(1-\sigma_{\mathrm{f}}\right)\varepsilon_{\mathrm{g}}\sigma-\frac{\sigma_{\mathrm{f}}\varepsilon_{\mathrm{f}}\varepsilon_{\mathrm{g}}\sigma}{\varepsilon_1}\right]\left(T_{\mathrm{g}}\right)_{\mathrm{m-1}}^4 \\
&\quad +sheatg\left(1-0.7\sigma_{\mathrm{f}}\right)T_{\mathrm{a}}+\rho_{\mathrm{ag}}C_{\mathrm{e}}^{\mathrm{g}}lW_{\mathrm{af}}M_{\mathrm{g}}\left(\frac{1-0.7\sigma_{\mathrm{f}}}{d_1}\right)q_{\mathrm{a}} \\
&\quad +\rho_{\mathrm{ag}}C_{\mathrm{e}}^{\mathrm{g}}lW_{\mathrm{af}}M_{\mathrm{g}}\left(\frac{0.1\sigma_{\mathrm{f}}M_{\mathrm{g}}}{d_1}-M_{\mathrm{g}}\right)\left[q_{\mathrm{g,\,sat}}\left(\left(T_{\mathrm{g}}\right)_{\mathrm{m-1}}\right)-\left(T_{\mathrm{g}}\right)_{\mathrm{m-1}}\left.\frac{\partial q_{\mathrm{g,\,sat}}}{\partial T_{\mathrm{g}}}\right|_{T_{\mathrm{g}}=\left(T_{\mathrm{g}}\right)_{\mathrm{m-1}}}\right] \\
&\quad +\rho_{\mathrm{ag}}C_{\mathrm{e}}^{\mathrm{g}}lW_{\mathrm{af}}M_{\mathrm{g}}\left(\frac{0.6\sigma_{\mathrm{f}}r''}{d_1}\right)\left[q_{\mathrm{f,\,sat}}\left(\left(T_{\mathrm{f}}\right)_{\mathrm{m-1}}\right)-\left(T_{\mathrm{f}}\right)_{\mathrm{m-1}}\left.\frac{\partial q_{\mathrm{f,\,sat}}}{\partial T_{\mathrm{f}}}\right|_{T_{\mathrm{f}}=\left(T_{\mathrm{f}}\right)_{\mathrm{m-1}}}\right] \\
c_2^{\mathrm{g}} &= 4\left[-\left(1-\sigma_{\mathrm{f}}\right)\varepsilon_{\mathrm{g}}\sigma-\frac{\sigma_{\mathrm{f}}\varepsilon_{\mathrm{f}}\varepsilon_{\mathrm{g}}\sigma}{\varepsilon_1}\right]\left(T_{\mathrm{g}}\right)_{\mathrm{m-1}}^3+\left(0.1\sigma_{\mathrm{f}}-1\right)sheatg \\
&\quad +\rho_{\mathrm{ag}}C_{\mathrm{e}}^{\mathrm{g}}lW_{\mathrm{af}}M_{\mathrm{g}}\left(\frac{0.1\sigma_{\mathrm{f}}M_{\mathrm{g}}}{d_1}-M_{\mathrm{g}}\right)\left.\frac{\partial q_{\mathrm{g,\,sat}}}{\partial T_{\mathrm{g}}}\right|_{T_{\mathrm{g}}=\left(T_{\mathrm{g}}\right)_{\mathrm{m-1}}}-\frac{\kappa_1}{\Delta z_1}-vc_{\mathrm{p}} \\
c_3^{\mathrm{g}} &= 4\frac{\sigma_{\mathrm{f}}\varepsilon_{\mathrm{f}}\varepsilon_{\mathrm{g}}\sigma}{\varepsilon_1}\left(T_{\mathrm{f}}\right)_{\mathrm{m-1}}^3+0.6\sigma_{\mathrm{f}}sheatg+\rho_{\mathrm{ag}}C_{\mathrm{e}}^{\mathrm{g}}lW_{\mathrm{af}}M_{\mathrm{g}}\left(\frac{0.6\sigma_{\mathrm{f}}r''}{d_1}\right)\left.\frac{\partial q_{\mathrm{f,\,sat}}}{\partial T_{\mathrm{f}}}\right|_{T_{\mathrm{f}}=\left(T_{\mathrm{f}}\right)_{\mathrm{m-1}}}
\end{aligned}
\tag{44}
$$

and

$$
\begin{aligned}
d_1 &= 1-\sigma_{\mathrm{f}}[0.6(1-r'')+0.1\left(1-M_{\mathrm{g}}\right)] \\
sheatf &= \left(e_0+1.1LAI\rho_{\mathrm{af}}c_{\mathrm{p,a}}C_{\mathrm{f}}W_{\mathrm{af}}\right) \\
sheatg &= \left(e_0+\rho_{\mathrm{ag}}c_{\mathrm{p,a}}C_{\mathrm{h}}^{\mathrm{g}}W_{\mathrm{af}}\right)
\end{aligned}
$$

This method is different from that originally used to solve for the surface temperature in FASST (Frankenstein and Koenig 2004). There, a fourth order equation was solved using a Newton-Raphson technique. This method is not used here because it does not allow for the simultaneous solution of T_{g} and T_{f}.

1.5 Root Uptake

Plants obtain moisture from both their leaves and roots. Thus, the soil moisture equations in Frankenstein and Koenig (2004) need to be modified. Following their nomenclature, the amount of water used at a single node is

$$\text{losses}(p) = 1.5 \times 10^{-7} \sigma_f \, ff \, \frac{R_p}{E_{tr,\,max}} \left[1 - \frac{\theta_p - \theta_r}{\theta_{max} - \theta_r} \right] \tag{45}$$

where R_p, $E_{tr,max}$ are defined in eq 20 and 28, respectively, and ff = 0.0 if the node is frozen, otherwise ff = 1.0.

1.6 Results

At the time of this work, there were no data sets available to the authors that measure the temperature gradient from above the foliage to the ground. Therefore, we chose to compare surface temperature and moisture and snow depth predictions for varying foliage densities. The data set chosen was collected in Grayling, Michigan, from mid-September through November 1992. The soil is a silty sand (SM). Based on photographs taken there, we used the "tall grass" vegetation type. Except for vegetation density, we used the default values for all other variables.

The peaks in soil moisture seen in Figure 3 result from rain. As the vegetation density increases, the soil response to storm events diminishes. Between storms, the greater vegetated surfaces exhibit less drying and diurnal fluxuations are also lost. The vegetation dampens the soil's response to evaporative forcing.

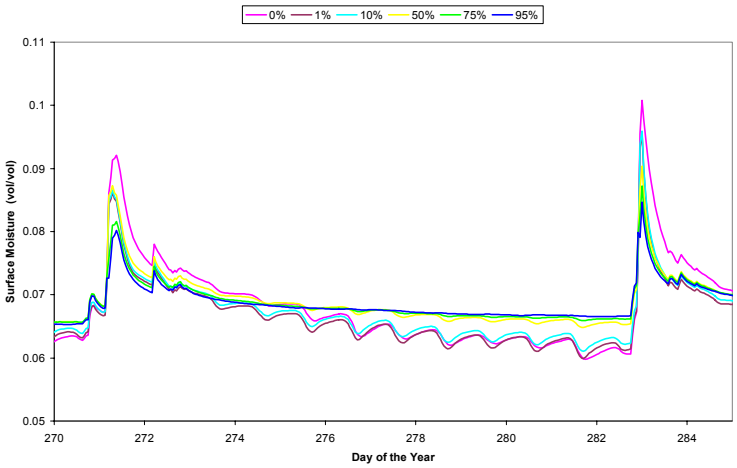

Figure 3. Soil moisture comparisons for Grayling, Michigan. Vegetation densities range from 0 to 95%. Vegetation type is "tall grass."

The vegetation has similar effects on the ground temperature, as can be seen in Figure 4. As the foliage density increases, the soil response to surface heating is dampened. Also, using the information shown in Figure 3, the wetter soil has lower maximums and higher minimums than the dryer soil.

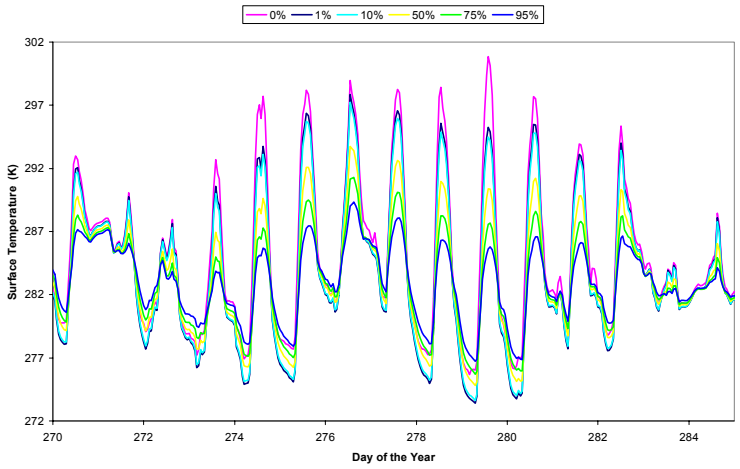

Figure 4. Soil temperature comparisons for Grayling, Michigan. Vegetation densities range from 0 to 95%. Vegetation type is "tall grass."

The variation in snow depth as a function of vegetation density is shown in Figure 5. It is difficult to discern any trends. During the first and third snow events, the snow took longer to melt in the bare ground scenario. The default grass height is 0.40 m in all cases. More studies are needed to better understand the relationship between vegetation density and snow accumulation.

Figure 6 investigates how the foliage temperature varies as a function of foliage density. Also shown on this figure is the air temperature above the foliage. The higher density grass is warmer than the lower density grass when it is dry. During precipitation events, the differences are mitigated. It is also seen in Figure 6 that, during the daytime, the air temperature and the foliage temperature are nearly the same during rain events, but that the air temperature is higher otherwise.

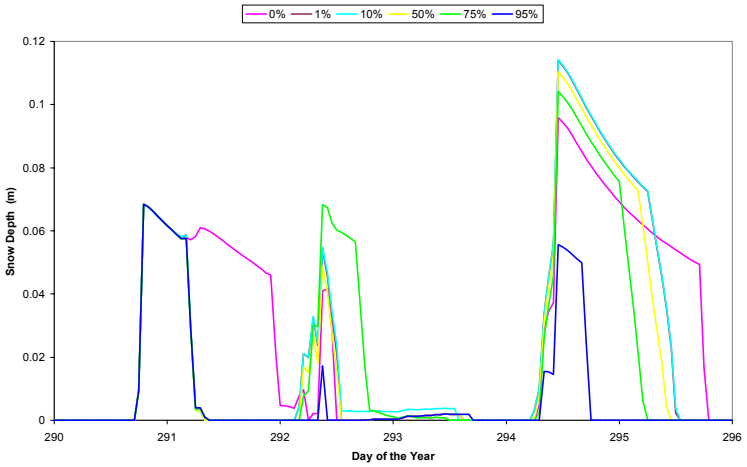

Figure 5. Snow depth comparisons for Grayling, Michigan. Vegetation densities range from 0 to 95%. Vegetation type is "tall grass."

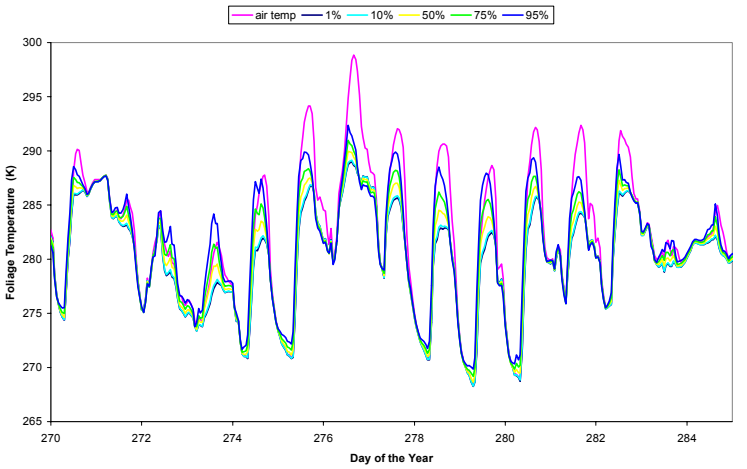

Figure 6. Foliage temperature comparisons for Grayling, Michigan. Vegetation densities range from 1–95%. Vegetation type is "tall grass."

2 HIGH VEGETATION MODEL—TREES/CANOPY

2.1 Introduction

The canopy model is based on the model developed by Smith et al. (1981) to investigate temperature and energy gradients within a forest. We chose this model as a starting point because we already possessed the code. It is a semi-infinite, steady-state plane parallel energy budget model consisting of three canopy layers, an atmospheric layer above the canopy, and a ground layer below the canopy. The model considers the longwave and shortwave fluxes and the interactions between the various layers, and uses the approach introduced in Section 1 for the canopy sensible heat, H_c, and evapotranspiration (latent heat), L_c, flux calculations. Unlike Smith et al. (1981), a precipitation heat term, P_c, is included in the canopy energy balance. The model also incorporates the orientation and distribution of leaves in the canopy layers.

2.2 Canopy Energy Model

The general form of the energy budget equation consisting of five sink (i) and five source (j) layers is given as

$$F_c = 0 = \sum_{i=1}^{3} \left[\begin{array}{l} A_c^i \left(I_{ir}^{\downarrow} S_{i1} + \sigma \sum_{j=2}^{4} \varepsilon_c^j \left(T_c^j \right)^4 S_{ij} + \varepsilon_g \sigma T_g^4 S_{i5} \right) - \sigma \varepsilon_c^i \left(T_c^i \right)^4 \sum_{k=1}^{5} S_{ki} \\ + a_c^i I_s^{\downarrow} + H_c^i + L_c^i - P_c^i \end{array} \right] \quad (46)$$

where the last term represents the precipitation heat, second and third terms on the second line represent the turbulent heat fluxes, the first term on the second line is the shortwave radiation flux, and the other terms capture the longwave radiation flux. ε_c^i, a_c^i and A_c^i are the canopy emissivity, and shortwave and longwave absorption coefficients of layer i, $I_{ir}^{\downarrow}$ (W/m^2) is the incoming longwave radiation, $I_s^{\downarrow}$ (W/m^2) is the incoming shortwave (solar) radiation, T_c^i (K) is the canopy layer i temperature, σ is the Stefan-Boltzman constant (5.699×10^{-8} W/m^2·K^4), and S_{ij} is the longwave transfer matrix between sink layer i and source layer j. Figure 7 depicts the schematic for the canopy model.

The longwave absorption coefficients are unique in that these coefficients are relative to the infrared flux at the top of the canopy rather than the infrared flux at the top of the individual canopy layers. The absorption coefficients are calculated using a Monte Carlo technique and include the effects of multiple scatter-

ing. Currently, the Monte Carlo technique used to compute the absorption coefficients is not part of the software. These coefficients for a needle leaf, broadleaf, and mixed canopy have been calculated using software developed by NASA.* These should not be changed without running a suitable radiative transfer or Monte Carlo model for the desired canopy geometrical and optical properties.

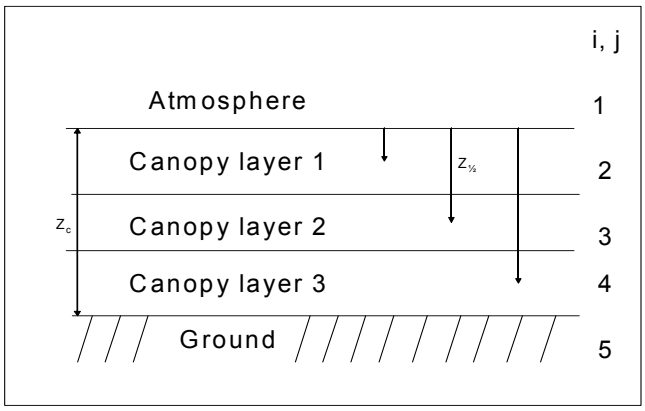

Figure 7. Source and sink layers for the canopy model.

2.2.1 Infrared Radiation

The atmospheric downwelling longwave (infrared) flux at the top of the canopy $I_{ir}^{\downarrow}$ absorbed by canopy layer *i* is $\varepsilon_c^i I_{ir}^{\downarrow} S_{i1}$. The longwave absorptivity is equal to the longwave emissivity ε_c^i and varies seasonally. The summer/winter values are 0.99/0.99, 0.97/0.90, and 0.98/0.94 for the top two layers for the needle leaf, broadleaf, and mixed leaf canopies, respectively. The lowest layer in all seasons, for all canopy types, is 0.90. $S_{i1}$is the longwave transfer matrix for the conveyance of atmospheric flux between the atmosphere (*j* = 1), the canopy layers (*i* = 2, 3, 4) and the ground (*i* = 5). The longwave flux emitted by canopy layer *j* $[\sigma\varepsilon_c^j \left(T_c^j\right)^4]$ or the ground ($\sigma\varepsilon_g T_g^4$) and absorbed by canopy layer *i*, is $\varepsilon_c^i\sigma\varepsilon_c^j \left(T_c^j\right)^4 S_{ij}$ for the canopy layer emitted flux and $\varepsilon_c^i\sigma\varepsilon_g T_g^4 S_{i5}$ for the ground emitted flux. Again, S_{i1} is the longwave transfer matrix for the flux emitted by canopy layer *j,* or the ground (*j* = 5), and absorbed by the other layers. The longwave transfer matrix is a function of C_{ijk}, the fraction of emitted flux from a source layer *j* that is intercepted by a foliage element $\hat{a}$ inclined at angle $d\theta_r$ within layer *i* (Smith and Goltz 1994) and is given as

* Personal communication with James Smith, National Aeronautics and Space Administration, 1994

$$S_{ij} = \sum_{k=1}^{9} C_{ijk} \tag{47}$$

The summation in eq 47 is over the leaf slope angle, θ_k , from 5.0 to 85.0 degrees in 10.0 degree increments. C_{ijk} is given as

$$C_{ijk} = \int_0^{\frac{\pi}{2}} \int_0^{2\pi} \left|\hat{a} \cdot \hat{r}\right| W_{ijr} d\theta_r d\phi_r \tag{48}$$

The weighting coefficients W_{ijr} are defined as

$$W_{1jr} = \begin{cases} 0 & j = 1 \\ \left[1 - P_0(j,r)\right] \prod_{k=i+1}^{j-1} P_0(k,r) & 2 \le j \le 4 \\ \prod_{k=i+1}^{j-1} P_0(k,r) & j = 5 \end{cases} \tag{49}$$

$$W_{5jr} = \begin{cases} \prod_{k=j+1}^{i-1} P_0(k,r) & j = 1 \\ \left[1 - P_0(j,r)\right] \prod_{k=j+1}^{i-1} P_0(k,r) & 2 \le j \le 4 \\ 0 & j = 5 \end{cases} \tag{50}$$

$$W_{ijr} = \begin{cases} P_0^{1/2}(i,r)\left[1 - P_0(j,r)\right] \prod_{k=i+1}^{j-1} P_0(k,r) & i < j \\ 2\left[1 - P_0^{1/2}(j,r)\right] & i = j \\ P_0^{1/2}(i,r)\left[1 - P_0(j,r)\right] \prod_{k=j+1}^{i-1} P_0(k,r) & i > j \end{cases} \tag{51}$$

where $2 \le i \le 4$ in eq 51 and $P_0(i,r)$ is the probability of gap for canopy layer i in direction $\hat{r}$. W_{ijr} is the flux contribution from source layer j to sink layer i for leaf distribution k for a source with a direction given by θ_r, ϕ_r and is expressed as the probability of gap when traversing a layer in direction $\hat{r}$. The unit vector $\hat{r}$ is

defined in terms of sin θ_r cos ϕ_r, sin θ_r sin ϕ_r, cos θ_r. The unit vector $\hat{a}$ in eq 48 represents the orientation of the foliage at leaf slope angle θ_k. The probability of gap, assuming no azimuthal dependence, is

$$P_0(i,r) = P_0(i,\theta_r) = \exp[LAI^i g(i,\theta_r) M^i \sec\theta_r] \tag{52}$$

where M^i is the Markov clumping factor (0 – 1). $g(i, \theta_r)$ is the mean layer projection in direction θ_r

$$g(i,\theta_r) = \int_0^{\frac{\pi}{2}} K(\theta_r,\theta_k) f_{ik} d\theta_k \tag{53}$$

There are a total of six leaf slope distribution functions, f_{ik}, (Verhoef and Bunnik 1975) available. These distributions are:

1. Planophile	$f_{ik} = 2/\pi\left[1+\cos(2\theta_k)\right]$	mostly horizontal
2. Erectophile	$f_{ik} = 2/\pi\left[1-\cos(2\theta_k)\right]$	mostly erect
3. Plagiophile	$f_{ik} = 2/\pi\left[1-\cos(4\theta_k)\right]$	mostly 45°
4. Extremophile	$f_{ik} = 2/\pi\left[1+\cos(4\theta_k)\right]$	mostly horizontal and vertical
5. Uniform	$f_{ik} = 2/\pi$	all possible inclinations
6. Spherical	$f_{ik} = \sin\theta_k$	mostly rounded

(54)

The kernel, $K(\theta_r, \theta_k)$ in eq 53 is defined as

$$K(\theta_r,\theta_k) = \begin{cases} \dfrac{2}{\pi}\cos\theta_k\cos\theta_r & \theta_k \le \dfrac{\pi}{2} - \theta_r \\ \left(\dfrac{2}{\pi}\right)^2 \cos\theta_k\cos\theta_r\left[\phi_k' - \dfrac{\pi}{2} - \tan\phi_k'\right] & \theta_k > \dfrac{\pi}{2} - \theta_r \end{cases} \tag{55}$$

and

$$\phi_k' = \cos^{-1}(-\cot\theta_k\cot\theta_r) \tag{56}$$

The Leaf Area Index LAI^{i} for each canopy layer is calculated in the same manner as for the low vegetation (see Section 1.2, eq 3). Default values for the minimum and maximum LAI^{i} are given in Table 3.

Table 3. Canopy properties.

Biome	$\sigma_{f,max}$* (%)	$\sigma_{f,min}$* (%)	LAI_{max}* (m^2/m^2)	LAI_{min}* (m^2/m^2)	SAI* (m^2/m^2)
evergreen needle-leaf	80	70	5.0	5.0	2.0
deciduous needle-leaf	80	50	6.0	1.0	2.0
deciduous broadleaf	80	50	6.0	1.0	2.0
evergreen broadleaf	90	40	6.0	5.0	2.0
mixed woodland	80	60	6.0	3.0	2.0

* Dickinson et al. (1986)

The term $A_c^i \varepsilon_g \sigma T_g^4 S_{i5}$ in eq 46 is the ground emitted longwave flux ($\varepsilon_g \sigma T_g^4$) that is transferred ($S_{i5}$) from the ground and is absorbed by the canopy layers (i = 2,3,4) and the atmosphere (i = 1). The calculation of the ground temperature T_g is described in Frankenstein and Koenig (2004) and in Section 1.4.

The canopy layer emitted flux, which represents a loss of energy from the canopy, is given as $-\sigma \varepsilon_c^i \left(T_c^i\right)^4$ in eq 46. The presence of a canopy modifies both the longwave and shortwave fluxes reaching the ground under the canopy. These modified fluxes are calculated from the measured fluxes at the top of the canopy, the canopy layer emitted fluxes, and the geometrical and optical properties of the canopy. The geometrical properties of the canopy are expressed in terms of the probability of gap and the probability of interception, as discussed above. The downwelling longwave flux at the ground, $I_{ir,g}^{\downarrow}$ underneath the canopy is given as

$$I_{ir,g}^{\downarrow} = I_{ir}^{\downarrow} S_{51} + \sigma \sum_{j=2}^{4} \varepsilon_j \left(T_c^j\right)^4 S_{5j} \tag{57}$$

This is taken as the incoming infrared radiation in eq 1 and 31 if a canopy layer is present. In other words, we can model any surface beneath a canopy layer.

2.2.2 Shortwave Radiation

The shortwave flux absorbed by canopy layer i is given as $a_c^i I_s^{\downarrow}$ where $I_s^{\downarrow}$ is the measured total solar flux at the top of the canopy. Expanded, it is written as (Smith and Goltz 1994)

$$a_c^i I_s^{\downarrow} = \left(1 - \Psi^i\right)\left[S_{i1} + \sum_{j=2}^{5} B_j S_{ij} \right] I_s^{\downarrow} \tag{58}$$

$$\Psi^i = \begin{cases} 1 - \left(Re^i + Tr^i \right) & i = 2,3,4 \\ \alpha_g & i = 5 \end{cases}$$

and Re^i and Tr^i are the canopy layer reflectance and transmittance respectively. α_g is the ground albedo as described earlier and B_j is the radiosity of layer j.

The total solar flux reaching the ground, $I_{s,g}^{\downarrow}$, under the canopy is given as

$$I_{s,g}^{\downarrow} = I_s^{\downarrow}\left(S_{51} + \sum_{j=2}^{4} B_j S_{5j} \right) \tag{59}$$

Similar to the longwave radiation reaching the ground beneath a canopy, this is taken as the incoming shortwave radiation in eq 1 and 31 if a canopy layer is present.

2.2.3 Sensible Heat Flux

Following the technique of Deardorff (1978) and Dickinson et al. (1986) as described in Section 1.2.2, the sensible heat flux (W/m^2) for canopy layer i is

$$H_c^i = \left(e_0 + 1.1 LAI^i \rho_{ac}^i c_{p,a} C_c^i W_{ac}^i \right)\left(T_{ac}^i - T_c^i \right) \tag{60}$$

where e_0, $c_{p,a}$ are as defined before. ρ_{ac}^i (kg/m^3), the air density at the air–canopy interface, is calculated using the ideal gas law, the atmospheric pressure, the air temperature at the air–canopy interface T_{ac}^i (K), and the canopy temperature T_c^i (K). The wind speed in the canopy, W_{ac}^i (m/s), is

$$W_{ac}^i = W' \exp\left(-1.1 \frac{Z_{1/2}^i}{Z_c} \right) \tag{61}$$

Z_c (m) and $Z_{1/2}^i$ (m) are defined in Figure 7 and W', the wind speed at the top of the canopy, is described in Section 1.2.2. C_c^i is calculated according to eq 10, replacing W_{af} with W_{ac}^i. Default values for parameters needed to calculate C_c^i are

given in Table 4. Following the method of Deardorf (1978), the air temperature in the canopy, T_{ac}^{i}, is given as

$$T_{ac}^{i} = \left(1-\sigma_{c}^{i}\right)T_{a}^{i} + \sigma_{c}^{i}\left(0.35T_{a}^{i} + 0.65T_{c}^{i}\right) \tag{62}$$

$$T_{a}^{i} = T_{a}\exp\left(0.05\frac{Z_{1/2}^{i}}{Z_{c}}\right) \tag{63}$$

For the first time step, the canopy layer temperatures are initialized to 90% of the air temperature. The air temperature and wind speed of the bottom layer are used as inputs in eq 1 and 31 if a canopy layer is present.

Table 4. Vegetation properties continued.

Biome	$r_{s,min}$* (s/m)	z_0^c* (m)	g_D† (10^{-2} Pa^{-1})	d_{max}** (mm)	a_r† (m^{-1})	b_r† (m^{-1})
evergreen needle-leaf	200	1.00	0.3	0.25	6.706	2.175
deciduous needle-leaf	200	1.00	0.3	0.10	7.066	1.953
deciduous broadleaf	200	0.80	0.3	0.10	7.344	1.303
evergreen broadleaf	150	2.00	0.3	0.25	5.990	1.955
mixed woodland	200	0.80	0.3	0.20	4.453	1.632

* Dickinson et al. (1986)
† http://www.ecmwf.int/research/ifsdocs/CY25r1/Physics/Physics-08-03.html
** Ramírez and Senarath (2000)

2.2.4 Latent Heat (Evapotranspiration) Flux

As for the sensible heat flux, the evapotranspiration is formulated following the method of Deardorff (1978) and introduced in Section 1.2.4. It is

$$L_{c}^{i} = LAI^{i}\rho_{ac}^{i}C_{c}^{i}lW_{ac}^{i}\left(r_{c}^{i}\right)''\left(q_{ac}^{i} - q_{c,\,sat}^{i}\right) \tag{64}$$

where

$$q_{ac}^{i} = \frac{\left(1-\sigma_{c}^{i}\right)q_{a}^{i} + \sigma_{c}^{i}\left(0.35q_{a}^{i} + 0.65\left(r_{c}^{i}\right)''q_{c,\,sat}^{i}\right)}{1-0.65\sigma_{c}^{i}\left[1-\left(r_{c}^{i}\right)''\right]} \tag{65}$$

In eq 64 l is the latent heat of evaporation (calculated according to eq 16) or sublimation depending on the temperature and $\left(r_c^i\right)''$ is the foliage wetness characterization. It is calculated using eq 17–22 making the appropriate substitutions and replacing the relative humidity, RH with

$$RH_c^i = 100 + \left(RH - 100\right)\exp\left(-5.5\frac{Z_{1/2}^i}{Z_c}\right) \tag{66}$$

The relative humidity of the bottom layer is used as input in eq 1 and 31 if a canopy layer is present.

2.2.5 Precipitation Heat Flux

The precipitation heat flux follows the same procedure outlined in Sections 1.2.4 and 1.3.4. For each canopy layer, it is

$$P_c^i = -\gamma_p \sigma_c^i \left[1.0 - \exp\left\{-0.5\left(LAI^i + SAI^i\right)\right\}\right] P_r^i c_p T_p \tag{67}$$

where $P_r^i = P_r$ for the top layer ($i = 2$) and $P_r^i = P_r^{i-1} - I^{i-1} + D^{i-1}$ for the lower layers ($i = 3, 4$). All terms are as described earlier.

2.3 Numerical Solution

Combining eq 46, 58, 60, and 64 gives the final form of the energy equation for the canopy

$$F_c = 0 = \sum_{i=1}^{3}\left[\begin{array}{l} A_c^i\left(I_{ir}^{\downarrow} S_{i1} + \sigma\sum_{j=2}^{4}\varepsilon_c^j\left(T_c^j\right)^4 S_{ij} + \varepsilon_g \sigma T_g^4 S_{i5}\right) - \sigma\varepsilon_c^i\left(T_c^i\right)^4\sum_{k=1}^{5} S_{ki} \\ +\left(1-\Psi_i\right)\left[S_{i1} + \sum_{j=2}^{5} B_j S_{ij}\right] I_s^{\downarrow} \\ -\left(e_0 + 1.1 LAI^i \rho_{ac}^i c_{p,a} C_c^i W_{ac}^i\right)\left(T_{ac}^i - T_c^i\right) - LAI^i \rho_{ac}^i C_c^i l W_{ac}^i \left(r_c^i\right)''\left(q_{ac}^i - q_{c,\,sat}^i\right) \\ +\gamma_p \sigma_c^i \left[1.0 - \exp\left\{-0.5\left(LAI^i + SAI^i\right)\right\}\right] P_r^i c_p T_p \end{array}\right] \tag{68}$$

Equation 68 is solved using an iterative Newton-Raphson technique (Burden et al. 1978).

2.4 Root Uptake

Quantification of water uptake by the canopy roots follows the procedure outlined in Section 1.5, eq 45, with σ_f replaced by σ_c, where σ_c is the maximum canopy density.

2.5 Results

As with the low vegetation model, we tested the high vegetation (canopy) model using data collected in Grayling, Michigan, during the fall of 1992. Again, only surface conditions were measured. Table 5 lists the input variables used. The values listed for foliage type, Markov clumping factor (M^i), shortwave absorption (a_c^i) and longwave emissivity (ε_c^i) are the values used for the SWOE (Smart Weapons Operability Enhancement) canopy studies carried out at Grayling, Michigan, for a deciduous forest (Welsh 1994). Our vegetation type is broadleaf deciduous. The mean canopy density varies between 50 and 80% (see eq 2).

Table 5. Canopy layer inputs for Grayling, Michigan, test.

Layer *i*	Foliage type	LAI^i	M^i	Thickness (m)	Re^i	Tr^i	A_c^i	ε_c^i
1	6	4.75	1.0	5.0	0.3	0.1	0.255	0.98
2	6	3.25	1.0	5.0	0.3	0.1	0.046	0.98
3	6	1.10	1.0	5.0	0.2	0.5	0.038	0.98

Figure 8 shows the surface soil moisture predictions with and without a forest canopy. The results are similar to the low vegetation results in that the soil is drier under the canopy when it rains but wetter between storms than the bare soil scenario. This is because some of the precipitation is being intercepted by the canopy, yet after the storm is over, the trees shelter the soil, decreasing surface evaporation. The tree roots also act to retain moisture in the soil. After day 290 in Figure 8, the bare soil case is wetter. This is caused by greater snow accumulation and thus greater snow melt infiltration in the absence of a canopy.

The soil surface under a canopy is, in general, warmer during the night and cooler or the same during the day as is seen in Figure 9. The diurnal variation is smaller under the canopy than for bare ground. This was also seen in the low vegetation scenario discussed in Section 1.6, although to a greater extent for the same foliage density. We believe that this is a result of the distance of the vegetation from the soil surface.

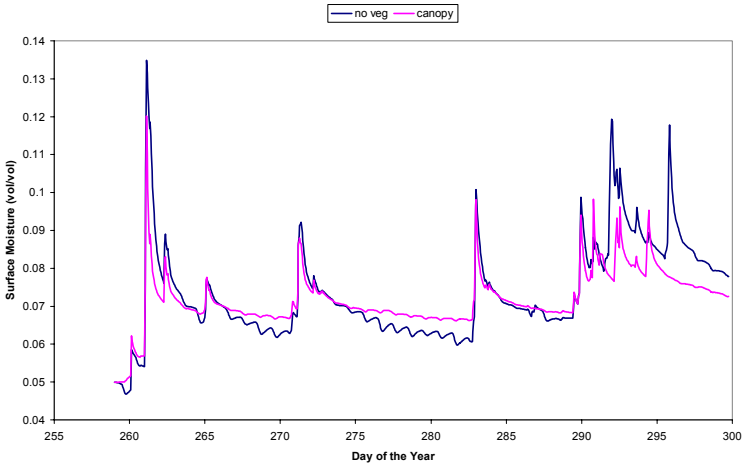

Figure 8. Comparison of surface moisture for the no vegetation case vs. a broadleaf deciduous canopy for Grayling, Michigan.

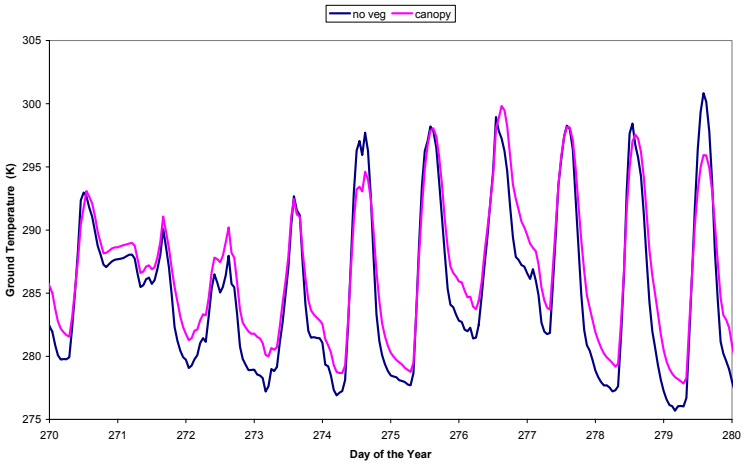

Figure 9. Comparison of surface temperature for the no vegetation case vs. a broadleaf deciduous canopy for Grayling, Michigan.

Figure 10 shows the temperature profile through the canopy, beginning with the air temperature above the canopy, then a representative top, middle, and bottom canopy temperature, and finally the soil surface temperature. Little difference is seen between the air temperature and the canopy temperatures, especially at night. During the peak daytime temperatures, there is approximately

1 K difference. The ground is noticeably warmer. The canopy appears to be acting as an insulator.

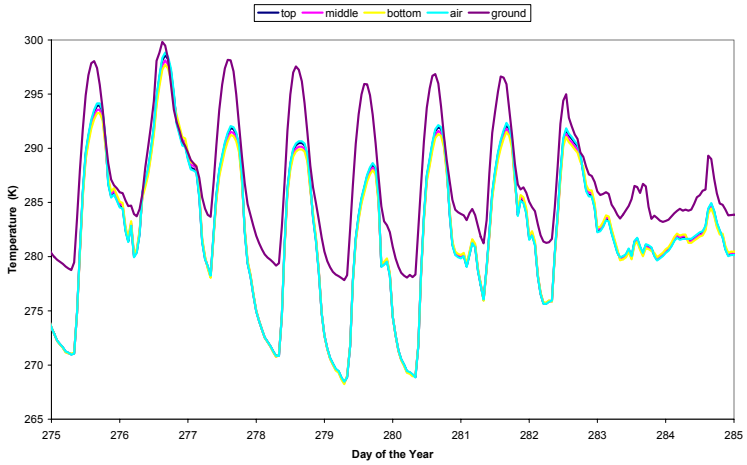

Figure 10. Temperature profile from above the canopy to the soil surface, including three canopy temperatures for Grayling, Michigan.

3 COMBINED LOW AND HIGH VEGETATION MODEL RESULTS

It is not uncommon for the forest floor to be covered with low vegetation. We, therefore, decided to run a simulation combining the broadleaf deciduous canopy with the tall grass scenes discussed in Sections 1.6 and 2.5. The low vegetation density is 78%. The results can be seen in Figures 11–14.

The most notable change when combining the canopy and grass layers in the soil moisture is the decreased soil moisture during storm events. As can be seen in Figure 11, this is almost entirely due to the low vegetation that intercepts much of the precipitation. As was previously seen, the roots tend to mitigate the diurnal variations and prevent the soil from drying to the extent of the bare soil case.

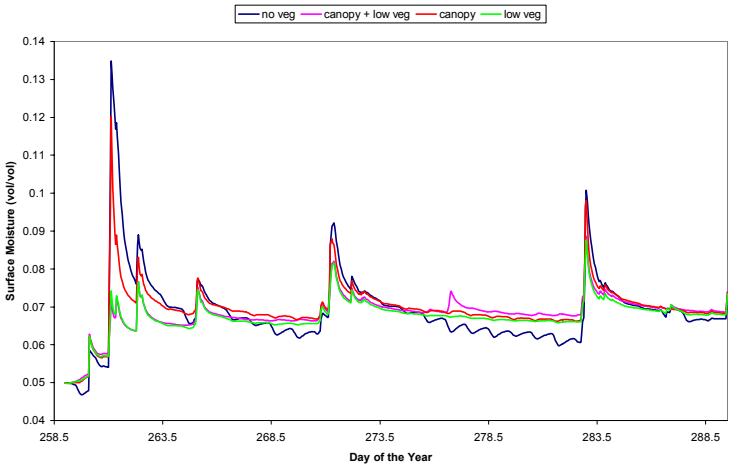

Figure 11. Soil moisture comparison for Grayling, Michigan.

Surface temperatures for each of the scenarios are shown in Figure 12. As with the soil moisture, the low vegetation appears to influence the soil temperature more than the canopy. For instance, on day 278 the maximum and minimum surface temperatures (K) for the bare soil, canopy only, low vegetation only, and combined forecasts are 296.78–277.69, 297.56–280.21, 287.53–277.71 and 290.34–279.33, respectively. This could be due to the proximity of the foliage to the soil and the presence of low clouds during the middle of the day (1300–1800 hours).

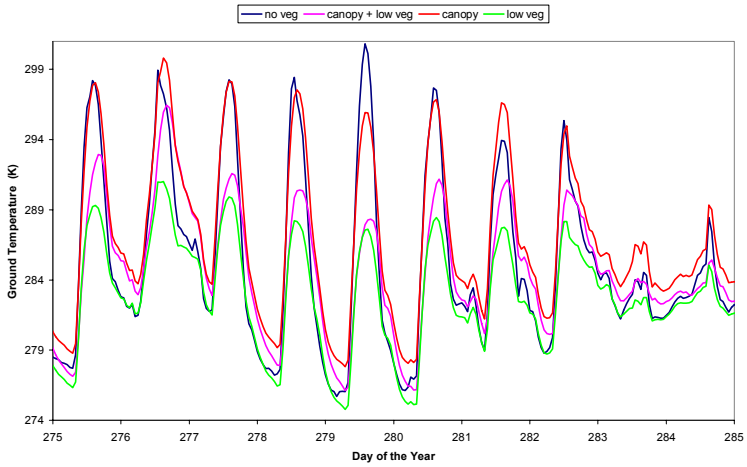

Figure 12. Soil surface temperature comparison for Grayling, Michigan.

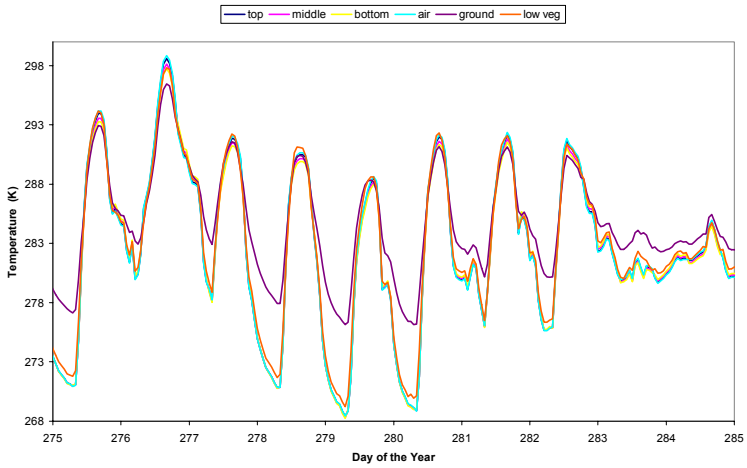

Figure 13. Temperature profile from above the canopy to the soil surface, including three canopy temperatures and a low vegetation temperature for Grayling, Michigan.

As with the canopy itself, the canopy and now grass temperatures closely follow the air temperature as is seen in Figure 13. One notable difference between Figures 10 and 13 is that the peak soil surfaces are much cooler in the combined scenario than in the tree only simulation. During the day, the ground surface temperature closely follows the air temperature, similar to the vegetation, but during the night the soil is warmer than the air. The only exception to this

occurs during rain events where the soil is warmer than the air and foliage during the day, as can be seen around day 283.

The disparity in snow depth seen in Figure 14 is due to the difference in soil surface temperature between the different scenarios. As the canopy simulation has the warmest soil, it has the least snow accumulation.

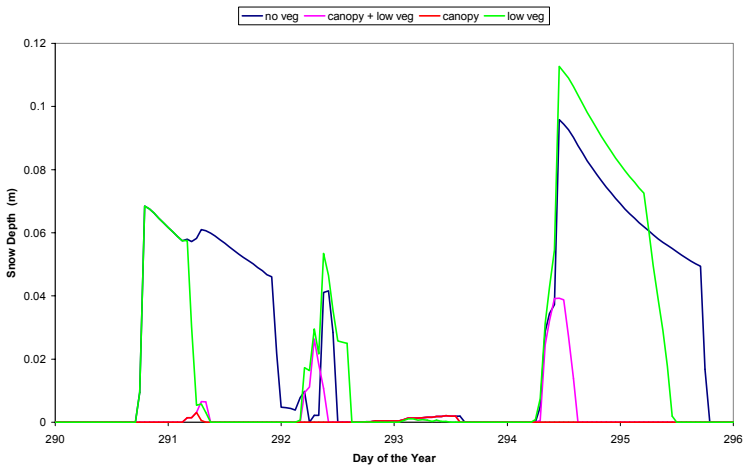

Figure 14. Snow depth comparison for Grayling, Michigan.

REFERENCES

Balick, L.K., L.E. Link, R.K. Scoggins, and J.L. Solomon (1981a) Thermal modeling of terrain surface elements. U.S. Army Engineer Waterways Experiment Station, Environmental Laboratory, Technical Repport, EL-81-2.

Balick, L.R., R.K. Scoggins, and L.E. Link (1981b) Inclusion of a simple vegetation layer in terrain temperature models for thermal IR signature prediction. *IEEE Geo. and Rem. Sens GE*, **19**(3): 143–152.

Buck, A. (1981) New equations for computing vapor pressure and the enhancement factor. *Journal of Applied Meteorology*, **20**(12): 1527–1532.

Burden, R.L., J.D. Faires, and A.C. Reynolds (1978) *Numerical Analysis*. Boston, Massachusetts: Prindle, Weber and Schmidt.

Chen, F., K. Mitchell, J. Schaake, Y. Xue, H.-L. Pan, V. Koren, Q. Yun Duan, M. Ek, and A. Betts (1996) Modeling of land surface evaporation by four schemes and comparison with FIFE observations. *Journal of Geophysical Research*, **101**(D3): 7251–7268.

Dai, Y., X. Zeng, and R.E. Dickinson (2001) *Common Land Model (CLM)—Technical Documentation and User's Guide.* http://www.eas.gatech.edu/dai/clmdoc.pdf.

Deardorff, J.W. (1978) Efficient prediction of ground surface temperature and moisture, with inclusion of a layer of vegetation. *Journal of Geophysical Research*, **83**(C4): 1889–1903.

Dickinson, R.E., A. Henderson-Sellers, P.J. Kennedy, and M.F. Wilson (1986) Biosphere-Atmosphere Transfer Scheme (BATS) for the NCAR community climate model. NCAR Technical Note, TN-275+STR.

European Centre for Medium-Range Weather Forecasts (ECMWF) (2002) *IFS (Integrated Forecast System) Documentation*, CY25R1 (Operational implementation 9 April 2002). http://www.ecmwf.int/research/ifsdocs/CY25r1/Physics/Physics-08-03.html.

Frankenstein, S., and G. Koenig (2004) Fast All-season Soil STrength (FASST). U.S. Army Engineer Research and Development Center, Cold regions Research and Engineering Laboratory, ERDC/CRREL Special Report SR-04-1.

Jordan, R. (1991) A one-dimensional temperature model for a snow cover: Technical documentation of SNTHERM.89. U.S. Army Cold Regions Research and Engineering Laboratory, Special Report 91-16.

Jordan, R. (1996) User's Guide for USACRREL one-Dimensional Snow Temperature Model (SNTHERM.89). U.S. Army Cold Regions Research and Engineering Laboratory.

Hughes, P.A., T.J.L. McComb, A.B. Rimmer, and K.E. Turver (1993) A mathematical model for the prediction of temperature of man-made and natural surfaces. *International Journal of Remote Sensing*, **14** (7): 1383–1412.

Kahle, A.B. (1977) A simple thermal model of the earth's surface for geologic mapping by remote sensing. Journal of Geophysical Research, **82** (11): 1673–1680.

Ramírez, J.A., and S.U.S. Senarath (2000) A statistical-dynamical parameterization of interception and land surface-atmosphere interactions. *Journal of Climate*, **13**(22): 4050–4063.

Sellers, P.J., Y. Mintz, Y.C. Sud, and A. Dalcher (1986) A simple biosphere model (SiB) for use within general circulation models. Journal of Atmospheric Science, **43**(6): 505–532.

Smith, J.A., and S.M. Goltz (1994) A thermal exitance and energy balance model for forest canopies. *IEEE Trans. On Geosci. And Remote Sensing*, **32**(5): 1060–1066.

Smith, J.A., and S.M. Goltz (1999) Simple forest canopy thermal-exitance model. *IEEE Trans. On Geosci. And Remote Sensing*, **37**(6): 2733–2736.

Smith, J.A., K.J. Ranson, D. Nguyen, L.K. Balick, L.E. Link, L. Fritchen, and B.A. Hutchison (1981) Thermal vegetation canopy model studies. *Remote Sensing of the Environment*, **11**: 311–326.

Tibbals, E.C., E.K. Carr, D.M. Gates, and F. Keith (1964) Radiation and convection in conifers. *American Journal of Botany*, **51**(5): 529–538.

Verhoef, W., and N.J.J. Bunnik (1975) A model study on the relations between crop characteristics and canopy spectral reflectance. NIWARS publications No. 33 (3). Kanaalweg Delft, The Netherlands.

Welsh, J.P. (1994) Smart Weapons Operability Enhancement (SWOE) Joint Test and Evaluation (JT&E) Program. SWOE Report 94-10.

APPENDIX A: DEFAULT MODEL VALUES

Table A1. Low Vegetation Model.

Variable	low	medium	high
$(1 - \alpha_f)_{min}$	0.70	0.70	0.70
$(1 - \alpha_f)_{max}$	0.85	0.85	0.85
$Z_{f,min}$ (cm)	5	35	85
$Z_{f,max}$ (cm)	50	60	85
$r_{s,max}$ (s/m)	500	500	500

$$\text{Variable} = \text{Variable}_{max} - (1.0 - f)(\text{Variable}_{max} - \text{Variable}_{min})$$

$$f = 1.0 - 0.016\left[298.0 - T_g\right]^2$$

Table A2. High Vegetation Model.

Variable	Evergreen Needle-leaf	Deciduous Needle-leaf	Evergreen Broadleaf	Deciduous Broadleaf	Mixed
Z_c (m)	25.5	36.0	21.0	31.5	30.0
layer thickness (m)	11.7 12.8 1.0	16.8 18.2 1.0	9.5 10.5 1.0	14.2 15.8 1.5	14.0 15.0 1.0
LAI factor	0.35 0.45 0.1	0.35 0.45 0.1	0.35 0.45 0.1	0.35 0.45 0.1	0.35 0.45 0.1
$r_{s,max}$ (s/m)	500	500	500	500	500
f_{ik}	6 6 6	6 6 6	6 6 6	6 6 6	6 6 6
M^i	0.5 0.5 1.0	0.5 0.5 1.0	0.5 0.5 1.0	0.5 0.5 1.0	0.5 0.5 1.0
a_c^i	0.229 0.214 0.079	0.229 0.214 0.079	0.255 0.046 0.038	0.255 0.046 0.038	0.242 0.130 0.058
ε_c^i : max, min	0.99, 0.99 0.99, 0.99 0.90, 0.90	0.99, 0.90 0.99, 0.90 0.90, 0.90	0.97, 0.90 0.97, 0.90 0.90 0.90	0.97, 0.97 0.97, 0.97 0.90, 0.90	0.98, 0.90 0.98, 0.90 0.90, 0.90

Variable	Evergreen Needle-leaf	Deciduous Needle-leaf	Evergreen Broadleaf	Deciduous Broadleaf	Mixed
Re^i :	0.28, 0.28	0.28, 0.21	0.28, 0.26	0.26, 0.26	0.28, 0.24
max, min	0.28, 0.28	0.28, 0.21	0.28, 0.26	0.26, 0.26	0.28, 0.24
	0.28, 0.28	0.28, 0.28	0.28, 0.28	0.28, 0.28	0.28, 0.28
Tr^i :	0.150, 0.150	0.150, 0.001	0.150, 0.001	0.150, 0.150	0.100, 0.001
min, max	0.150, 0.150	0.150, 0.001	0.150, 0.001	0.150, 0.150	0.100, 0.001
	0.001, 0.001	0.001, 0.001	0.001, 0.001	0.001, 0.001	0.001, 0.001

$$LAI^i = \sigma_f \left(LAI\ factor \right)$$

$$\varepsilon_c^i ,\ Tr^i = \text{Variable}_{max} - (1.0 - f)(\text{Variable}_{max} - \text{Variable}_{min})$$

$$Re^i = \text{Variable}_{min} + (1.0 - f)(\text{Variable}_{max} - \text{Variable}_{min})$$

$$f = 1.0 - 0.016\left[298.0 - T_g \right]^2$$

REPORT DOCUMENTATION PAGE

Form Approved
OMB No. 0704-0188

1. REPORT DATE *(DD-MM-YYYY)*	2. REPORT TYPE	3. DATES COVERED *(From - To)*
December 2004		

4. TITLE AND SUBTITLE

FASST Vegetation Models

5a. CONTRACT NUMBER

5b. GRANT NUMBER

5c. PROGRAM ELEMENT NUMBER

6. AUTHOR(S)

S. Frankenstein and G. Koenig

5d. PROJECT NUMBER

5e. TASK NUMBER

5f. WORK UNIT NUMBER

7. PERFORMING ORGANIZATION NAME(S) AND ADDRESS(ES)

Engineer Research and Development Center
Cold Regions Research and Engineering Laboratory
72 Lyme Road
Hanover, New Hampshire 03755

8. PERFORMING ORGANIZATION REPORT NUMBER

ERDC/CRREL TR-04-25

9. SPONSORING / MONITORING AGENCY NAME(S) AND ADDRESS(ES)

U.S. Army Corps of Engineers
Washington, DC 20314-1000

10. SPONSOR/MONITOR'S ACRONYM(S)

11. SPONSOR/MONITOR'S REPORT NUMBER(S)

12. DISTRIBUTION / AVAILABILITY STATEMENT

Approved for public release; distribution is unlimited

13. SUPPLEMENTARY NOTES

14. ABSTRACT

The one-dimensional dynamic state of the ground model FASST (Fast All-season Soil Strength) is a state of the ground model developed by Frankenstein and Koenig (2004) as part of the Army's Battlespace Terrain Reasoning and Awareness (BTRA) research program. In its original form, the only effects vegetation had on FASST were to change the surface albedo and emissivity. Recently, a two tier, multilayer vegetation algorithm was added. These can be implemented separately or together. Both alter the soil surface energy and moisture budgets. In this report we will discuss the energy balance equations used to solve for the low vegetation, canopy and ground temperatures. In solving these equations, the effects of precipitation interception and soil moisture modification attributable to root-uptake are incorporated.

15. SUBJECT TERMS

Canopy
Foliage moisture
Foliage temperature
Low vegetation
Root uptake

16. SECURITY CLASSIFICATION OF:			17. LIMITATION OF ABSTRACT	18. NUMBER OF PAGES	19a. NAME OF RESPONSIBLE PERSON
a. REPORT	b. ABSTRACT	c. THIS PAGE			19b. TELEPHONE NUMBER *(include area code)*
Unclassified	Unclassified	Unclassified	Unclassified	56	

Standard Form 298 (Rev. 8-98)
Prescribed by ANSI Std. 239.18